Supporting Information

Personalized Keystroke Dynamics for Self-Powered Human-Machine Interfacing

*Jun Chen,[†,⊥] Guang Zhu,[†§⊥] Jin Yang,[†‡⊥] Qingshen Jing,[†] Peng Bai,[†] Weiqing Yang,[†] Xuewei Qi,[#] Yuanjie Su,[†] Zhong Lin Wang[†,§]**

[†] School of Materials Science and Engineering, Georgia Institute of Technology, Atlanta. GA 30332-0245, United States.

[§] Beijing Institute of Nanoenergy and Nanosystems, Chinese Academy of Sciences, Beijing 100083,
China.

[‡] Department of Optoelectronic Engineering, Chongqing University, Chongqing 400044, China.

[#] Department of Electrical Engineering, University of California, Riverside, CA, 92521, USA.

[⊥] Authors with equal contribution.

*Correspondence to: zhong.wang@mse.gatech.edu

Keywords: triboelectrification, IKB, self-powering, human-machine interfacing, keystroke dynamics, biometrics.

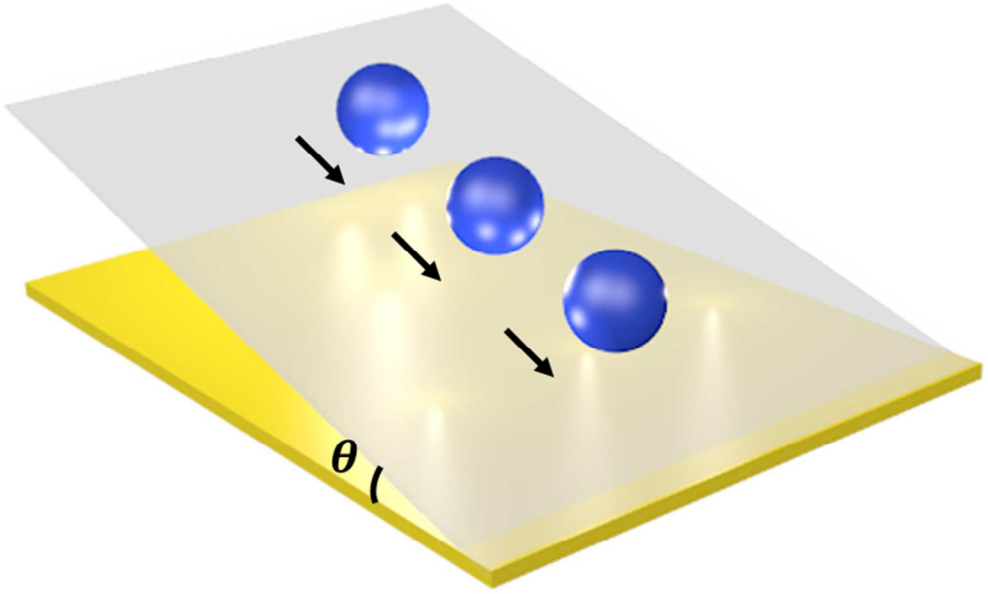

Supporting Figure S1 | Tilting base method for surface sliding angle measurement. It graphically shows the sliding angle measurement using a tilting base method.

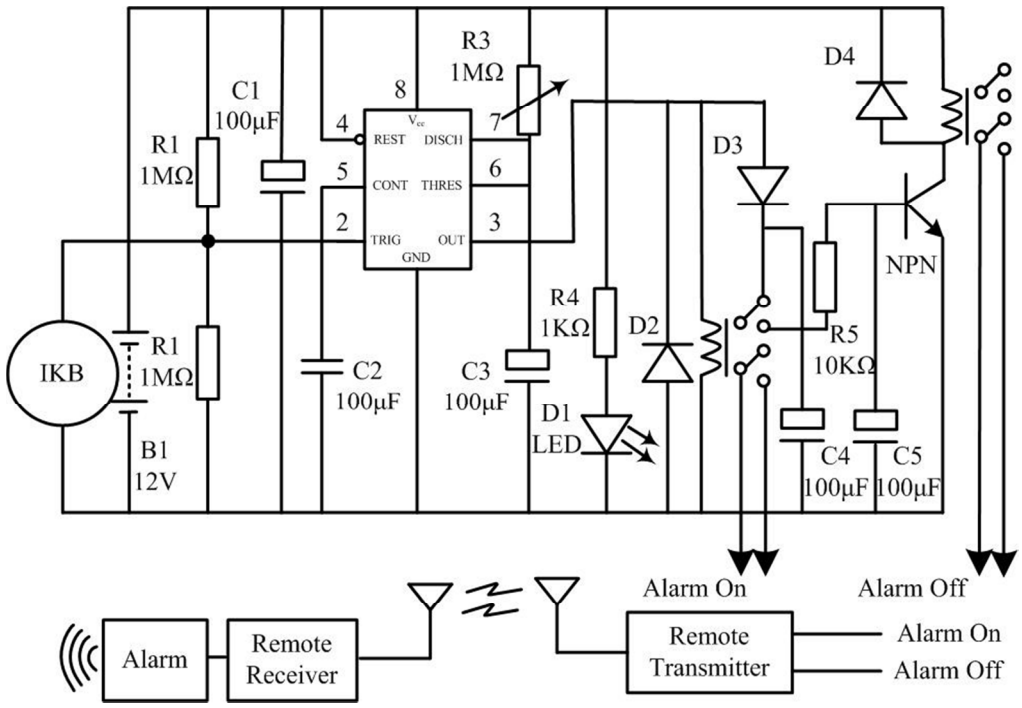

Supporting Figure S2 | Circuit diagram of the complete self-securing system. It consists of an IKB and a signal processing circuit.

Supporting Figure S3 | Keys classification in the intelligent keyboard. The keys in the keyboards are classified into seven kinds according to their dimensions.

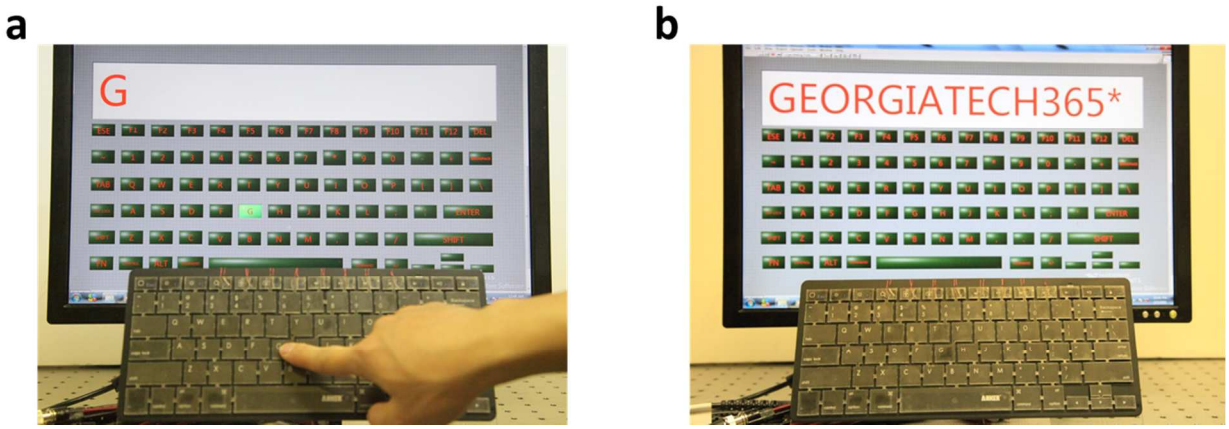

Supporting Figure S4 | Intelligent keyboard as a self-securing system to trace and record the typing motions. When a string "GEORGIATECH365*" was continuously typed on the intelligent keyboard, it was successfully recorded without uncomfortable delay.

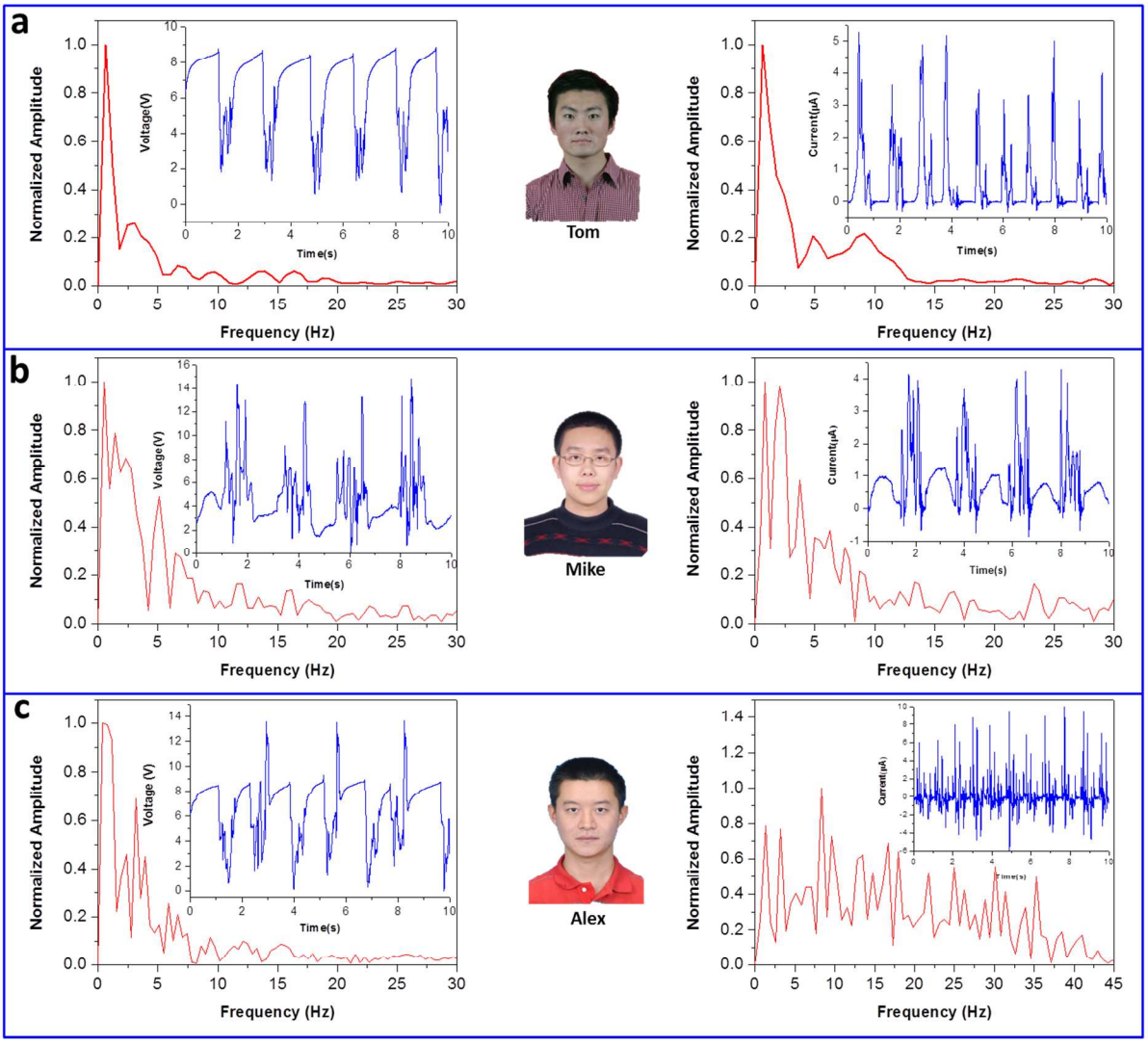

Supporting Figure S5| Frequency spectrums of the typing patterns obtained from the intelligent keyboard. Frequency spectrum of the voltage and current signals, which was obtained when (**a**)Tom, (**b**) Mike, (**c**)Alex, was continuously tying the word "touch" more than four times into the computer *via* the intelligent keyboard. Inset: their corresponding original typing patterns. As shown, the frequency spectrums are different from each other in term of the positions and amplitudes of the major components of the signals.

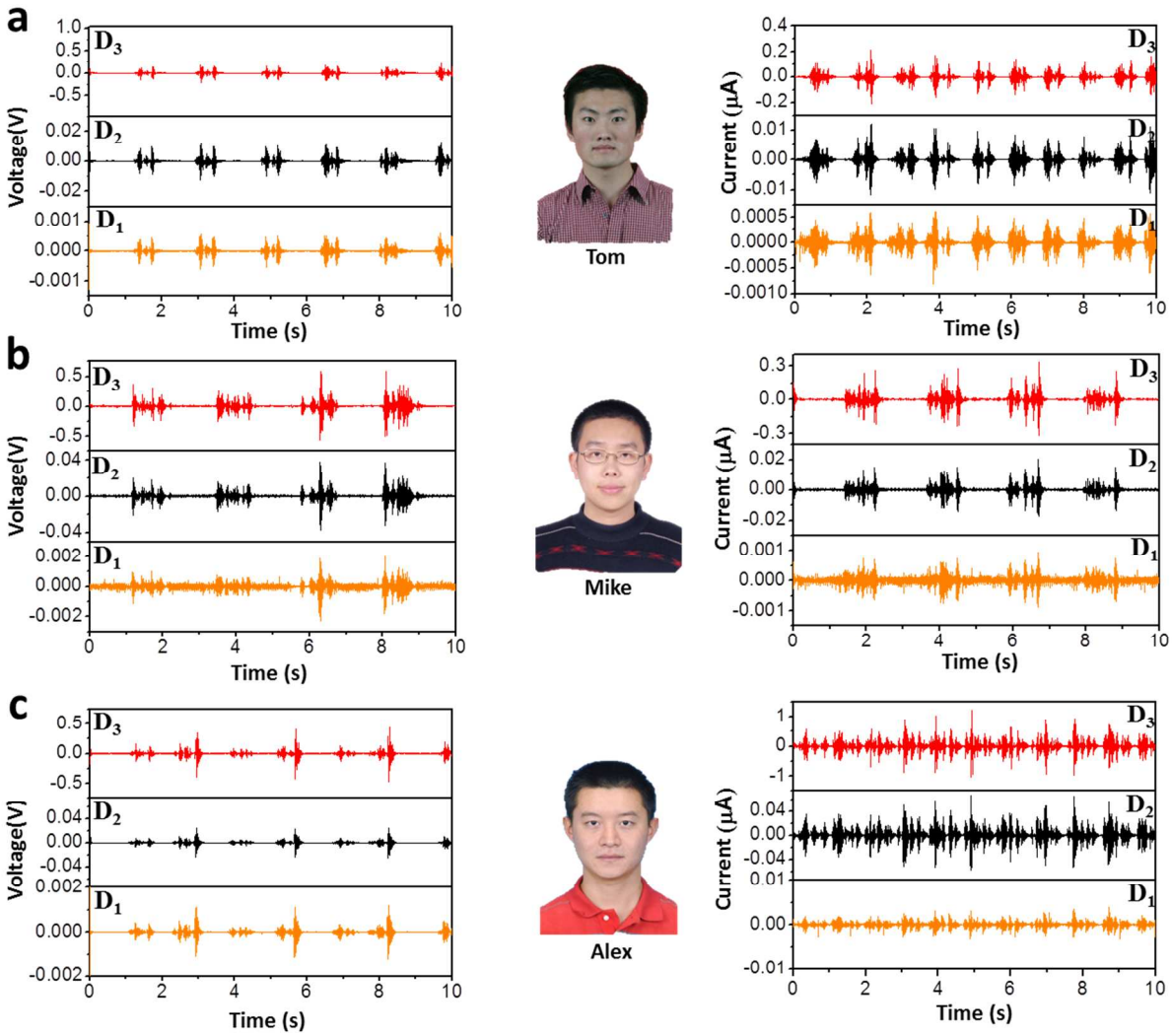

Supporting Figure S6| The typing patterns after Daubechies Wavelet of order 4 (DB4) transformation. The higher resolution terms D_3, D_2, D_1 of original typing patterns after DB4 transformation, respectively for (**a**)Tom, (**b**)Mike and (**c**)Alex. As shown, these higher resolution wavelet components of the typing patterns are significantly different from each other.

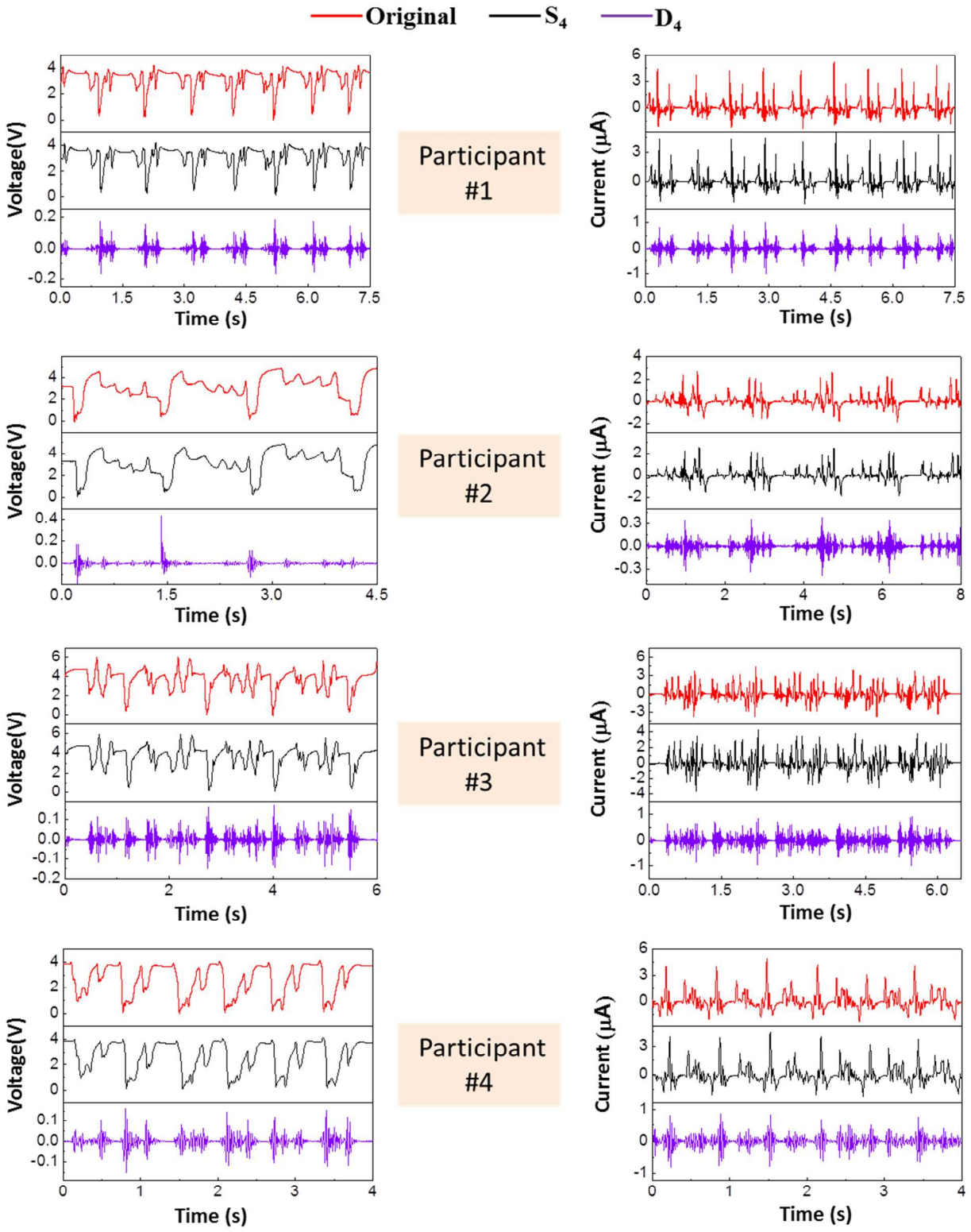

Supporting Figure S7| The typing patterns of participants 1 to 4. Typing patterns obtained when they were continuously tying the word "touch" into the computer *via* the IKB. S_4 and D_4 are the corresponding wavelet components after DB4 transformation.

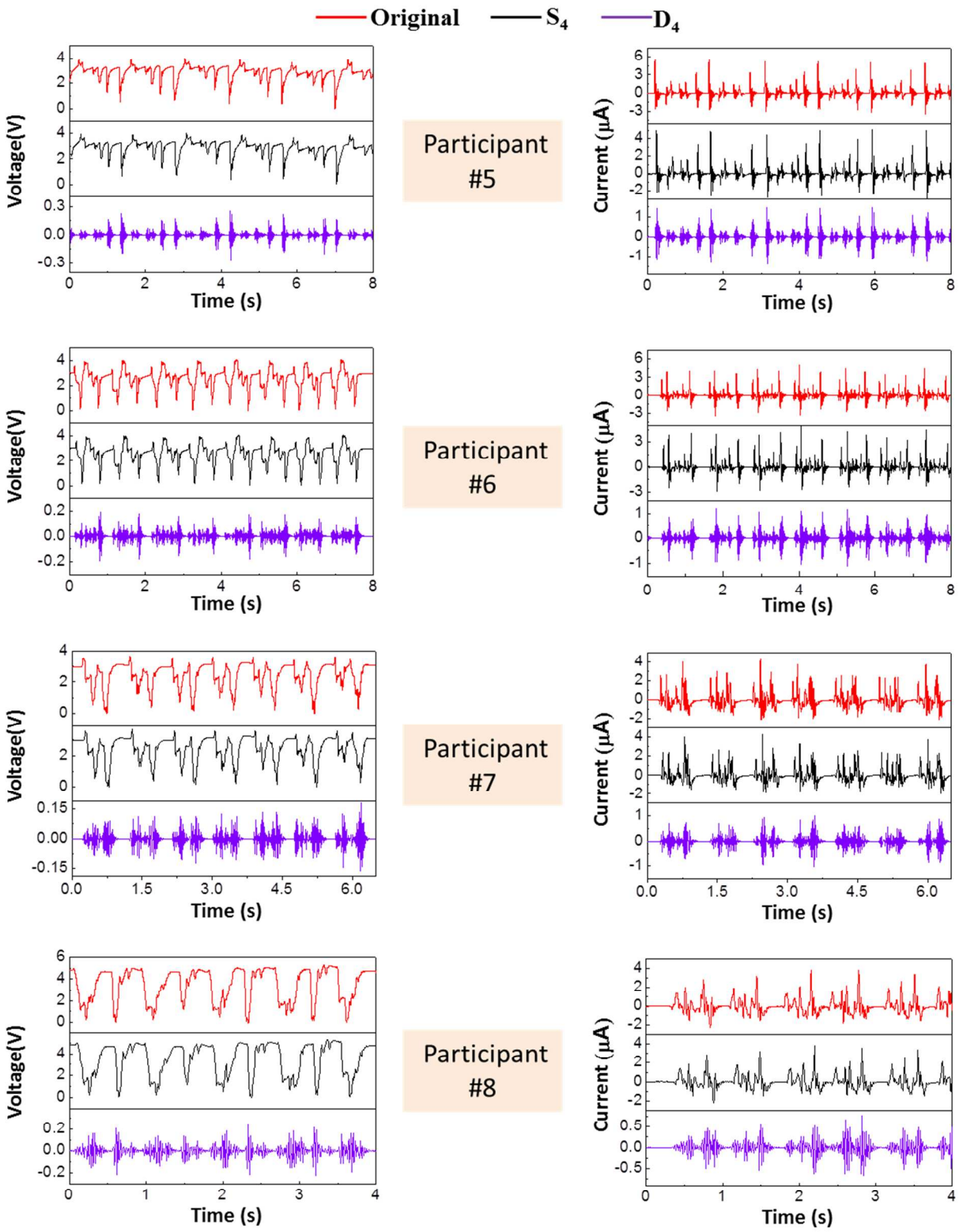

Supporting Figure S8| The typing patterns of participants 5 to 8. Typing patterns obtained when they were continuously tying the word "touch" into the computer *via* the IKB. S_4 and D_4 are the corresponding wavelet components after DB4 transformation.

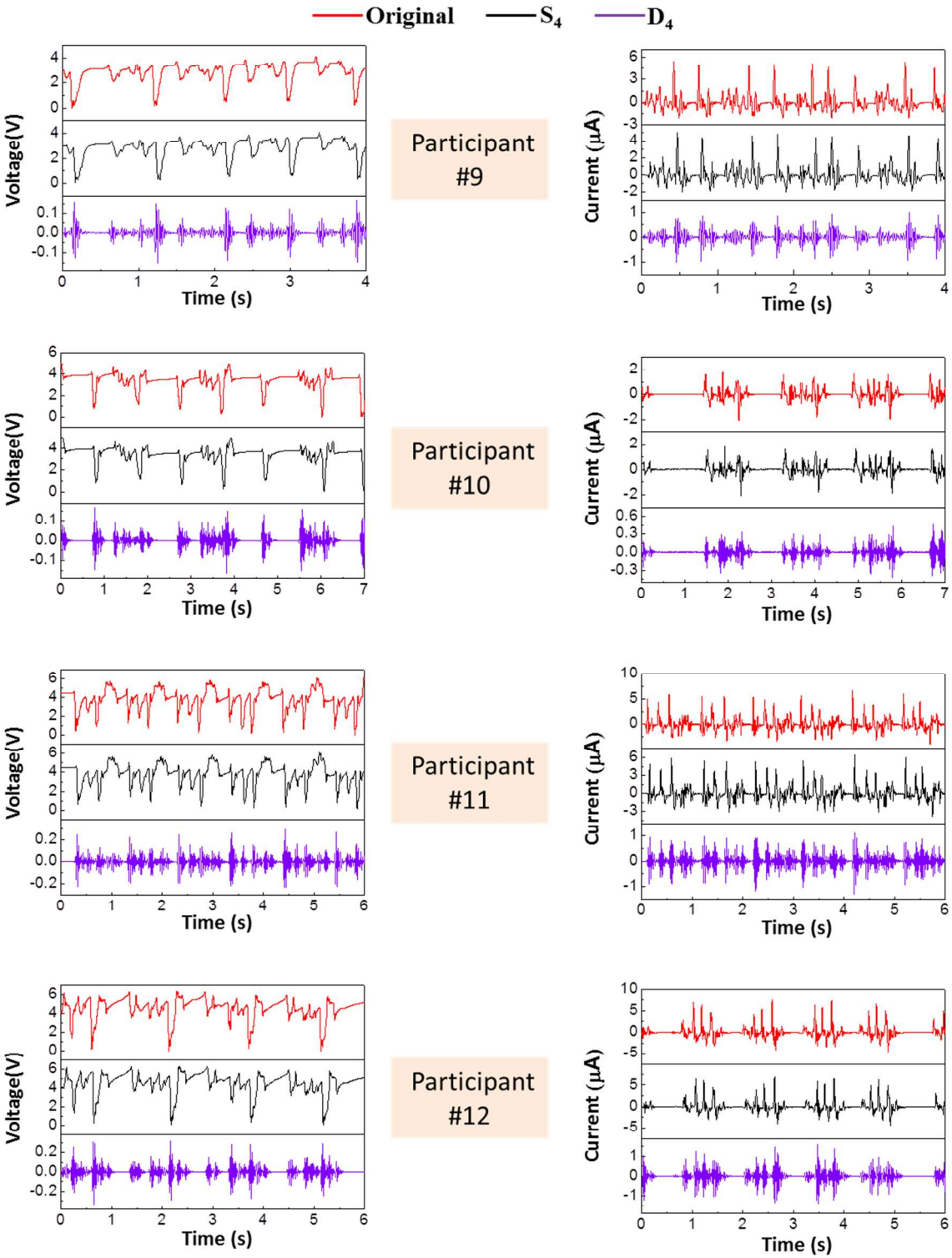

Supporting Figure S9| The typing patterns of participants 9 to 12. Typing patterns obtained when they were continuously tying the word "touch" into the computer *via* the IKB. S_4 and D_4 are the corresponding wavelet components after DB4 transformation.

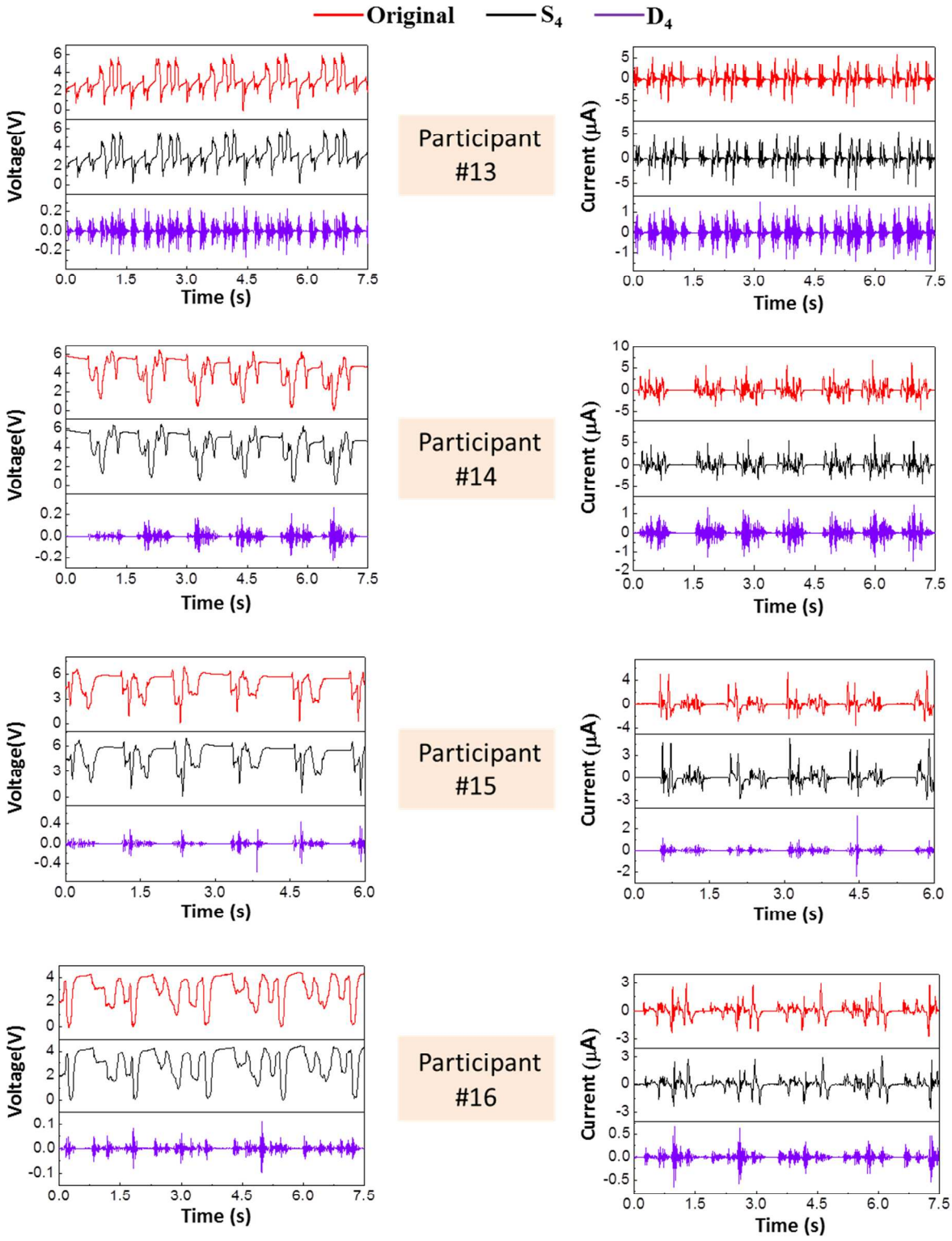

Supporting Figure S10| The typing patterns of participants 13 to 16. Typing patterns obtained when they were continuously tying the word "touch" into the computer *via* the IKB. S_4 and D_4 are the corresponding wavelet components after DB4 transformation.

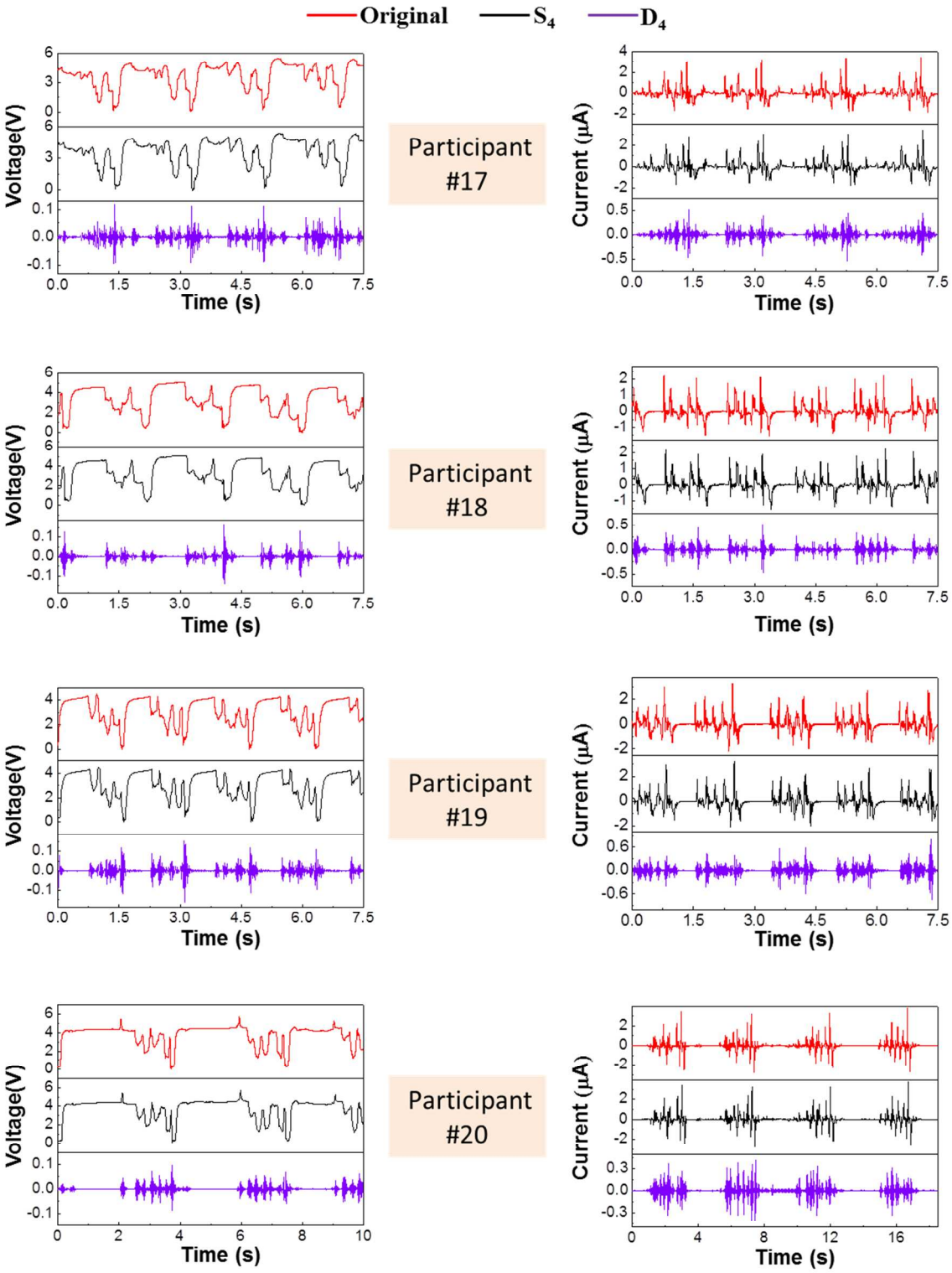

Supporting Figure S11 | The typing patterns of participants 17 to 20. Typing patterns obtained when they were continuously tying the word "touch" into the computer *via* the IKB. S_4 and D_4 are the corresponding wavelet components after DB4 transformation.

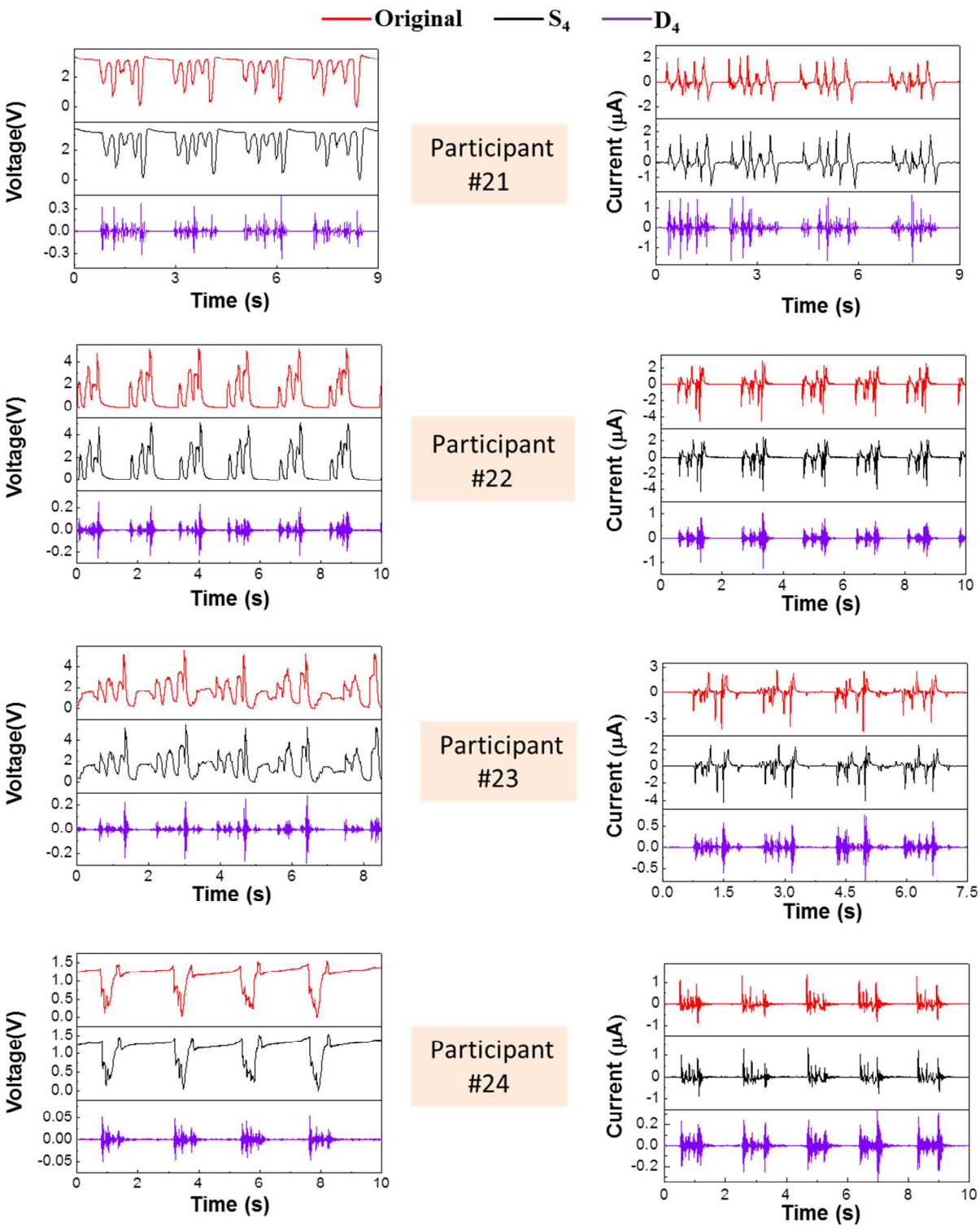

Supporting Figure S12 | The typing patterns of participants 21 to 24. Typing patterns obtained when they were continuously tying the word "touch" into the computer *via* the IKB. S_4 and D_4 are the corresponding wavelet components after DB4 transformation.

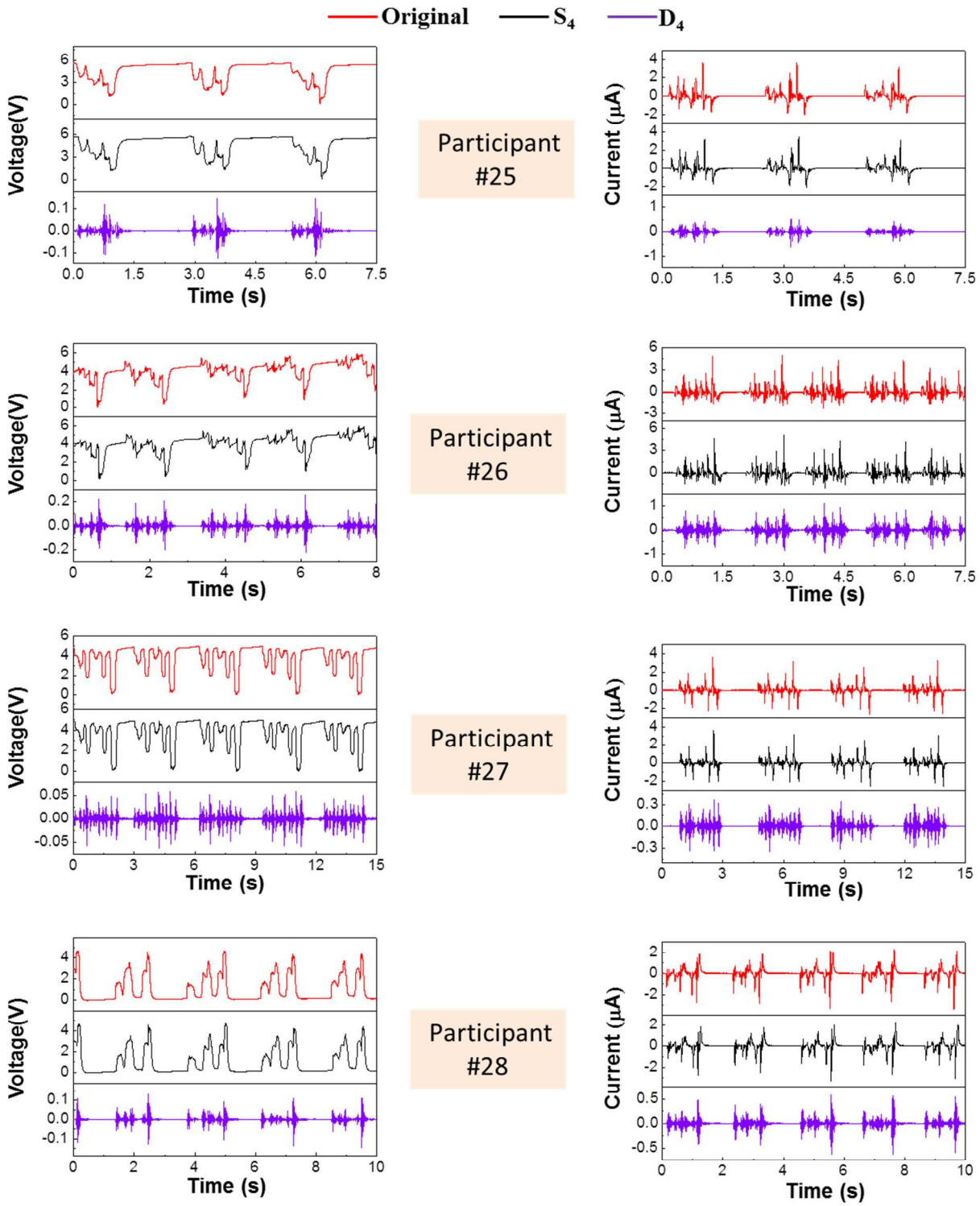

Supporting Figure S13 | The typing patterns of participants 25 to 28. Typing patterns obtained when they were continuously tying the word "touch" into the computer *via* the IKB. S_4 and D_4 are the corresponding wavelet components after DB4 transformation.

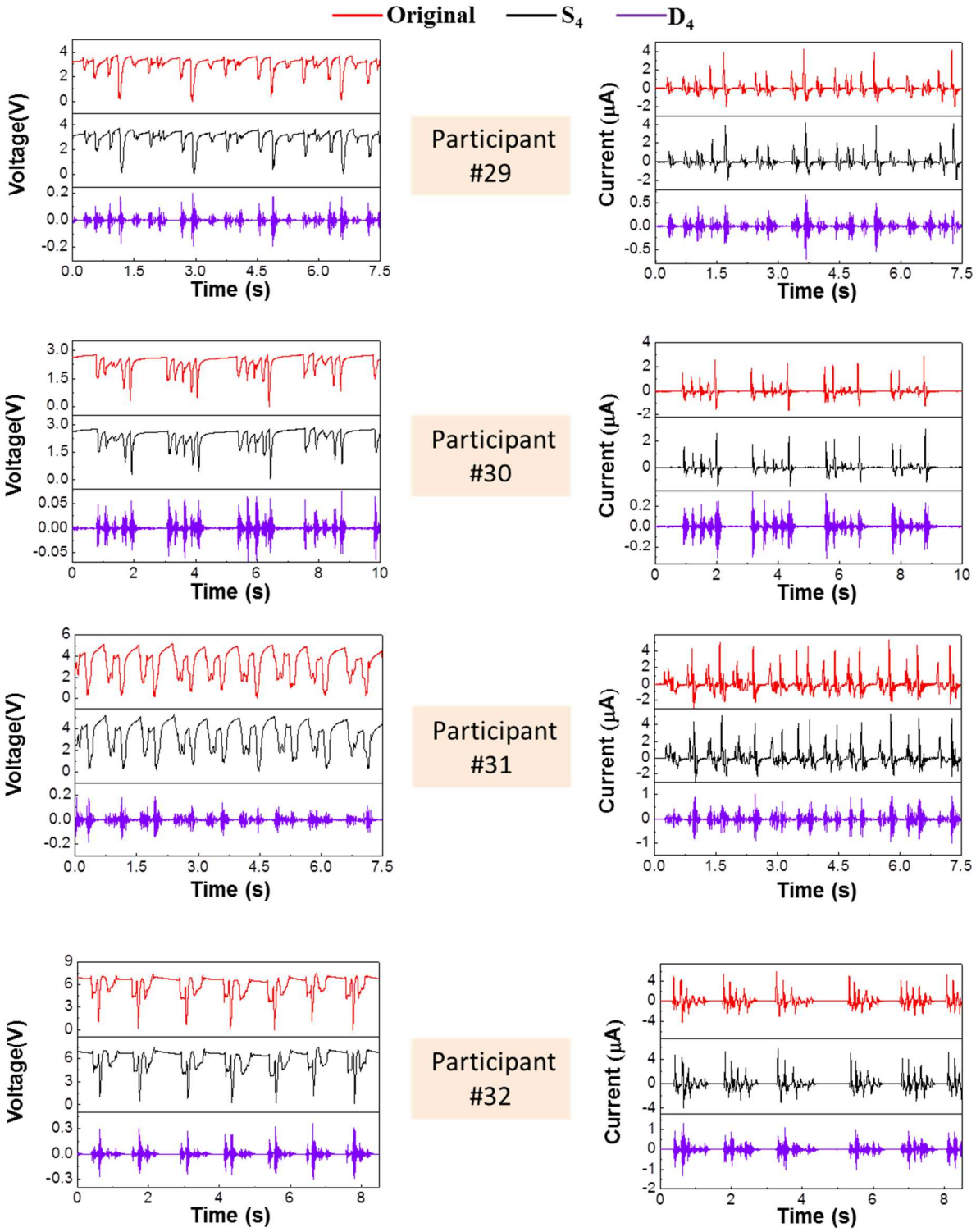

Supporting Figure S14 | The typing patterns of participants 29 to 32. Typing patterns obtained when they were continuously tying the word "touch" into the computer *via* the IKB. S_4 and D_4 are the corresponding wavelet components after DB4 transformation.

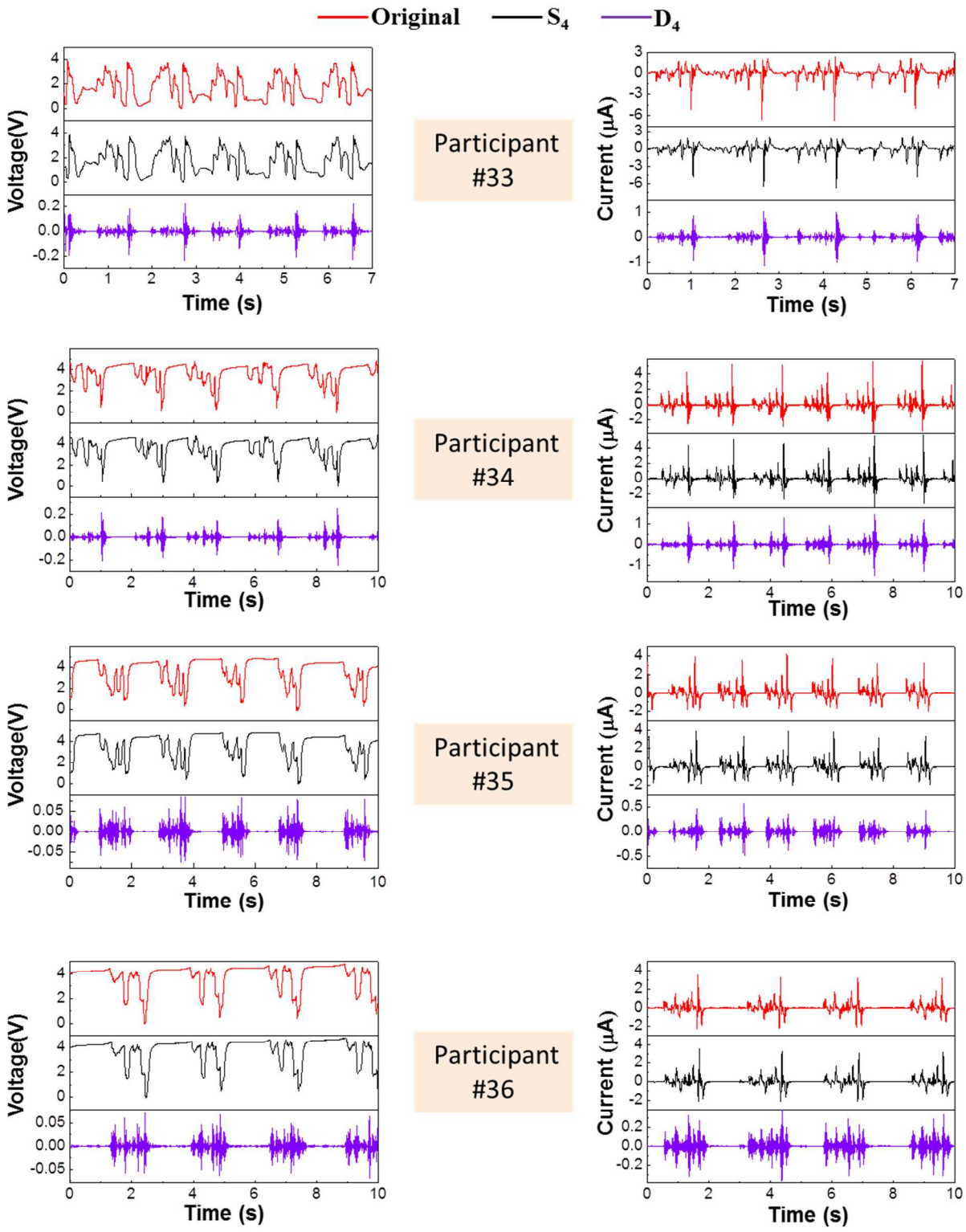

Supporting Figure S15 | The typing patterns of participants 33 to 36. Typing patterns obtained when they were continuously tying the word "touch" into the computer *via* the IKB. S_4 and D_4 are the corresponding wavelet components after DB4 transformation.

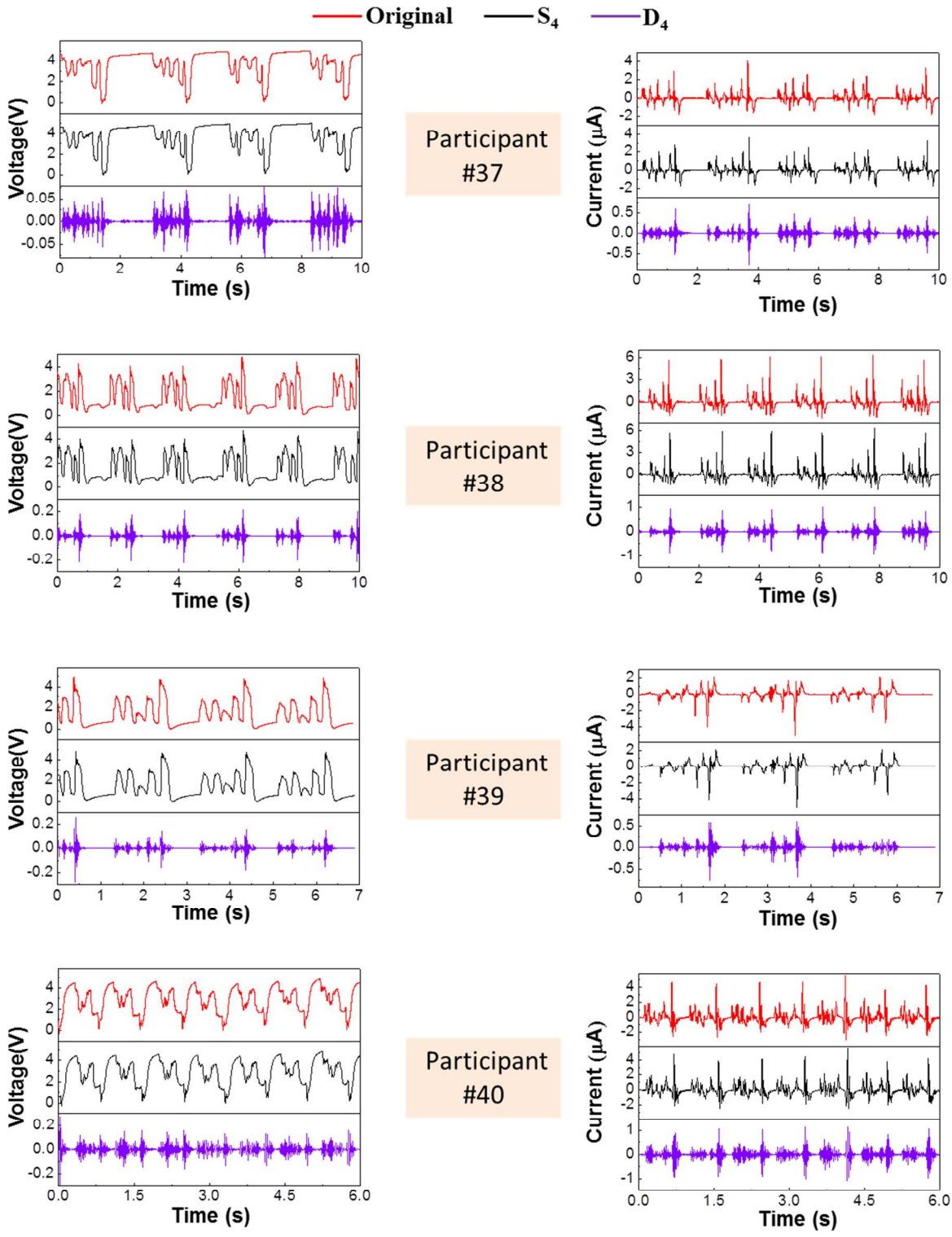

Supporting Figure S16 | The typing patterns of participants 37 to 40. Typing patterns obtained when they were continuously tying the word "touch" into the computer *via* the IKB. S_4 and D_4 are the corresponding wavelet components after DB4 transformation.

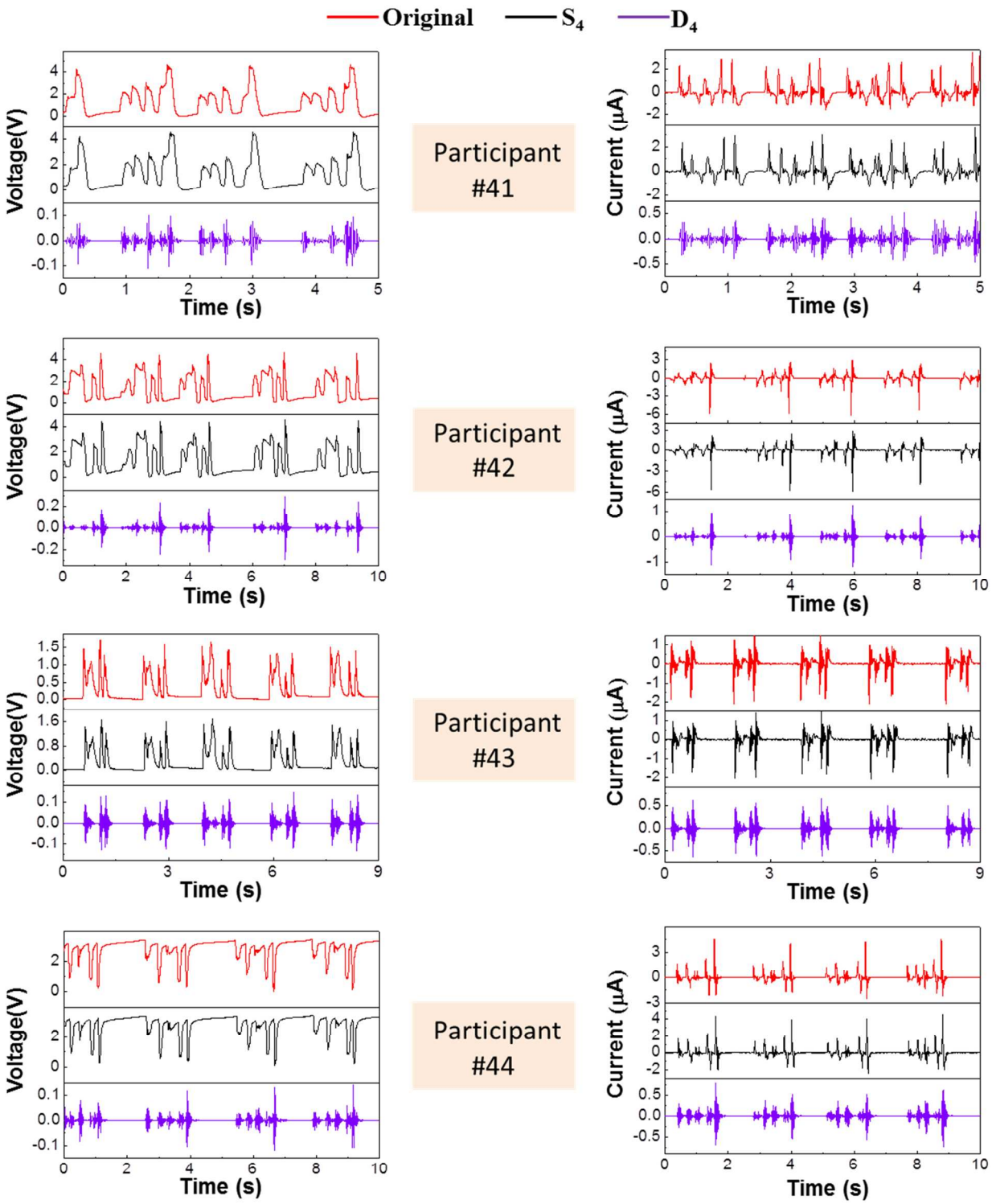

Supporting Figure S17 | The typing patterns of participants 41 to 44. Typing patterns obtained when they were continuously tying the word "touch" into the computer *via* the IKB. S_4 and D_4 are the corresponding wavelet components after DB4 transformation.

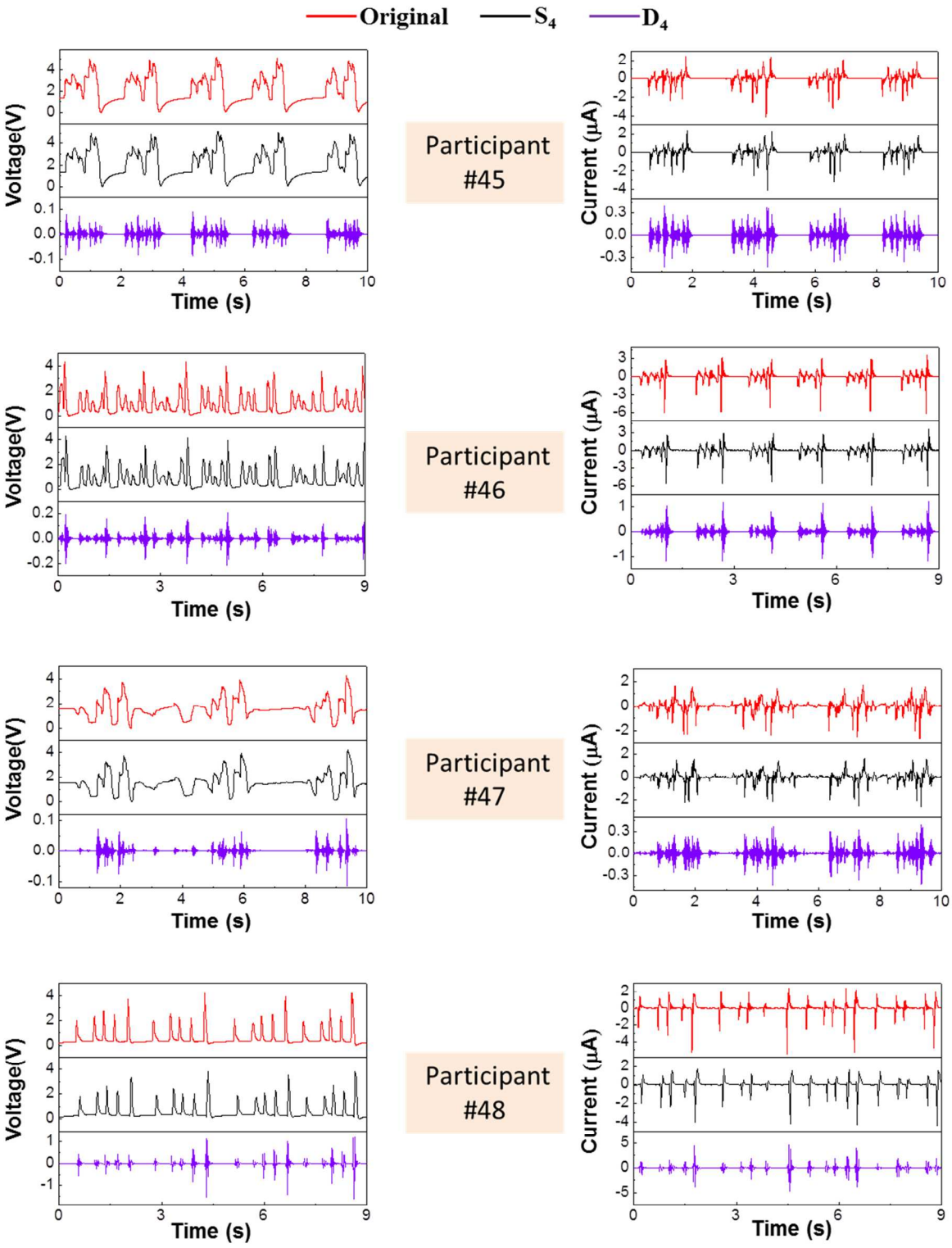

Supporting Figure S18 | The typing patterns of participants 45 to 48. Typing patterns obtained when they were continuously tying the word "touch" into the computer *via* the IKB. S_4 and D_4 are the corresponding wavelet components after DB4 transformation.

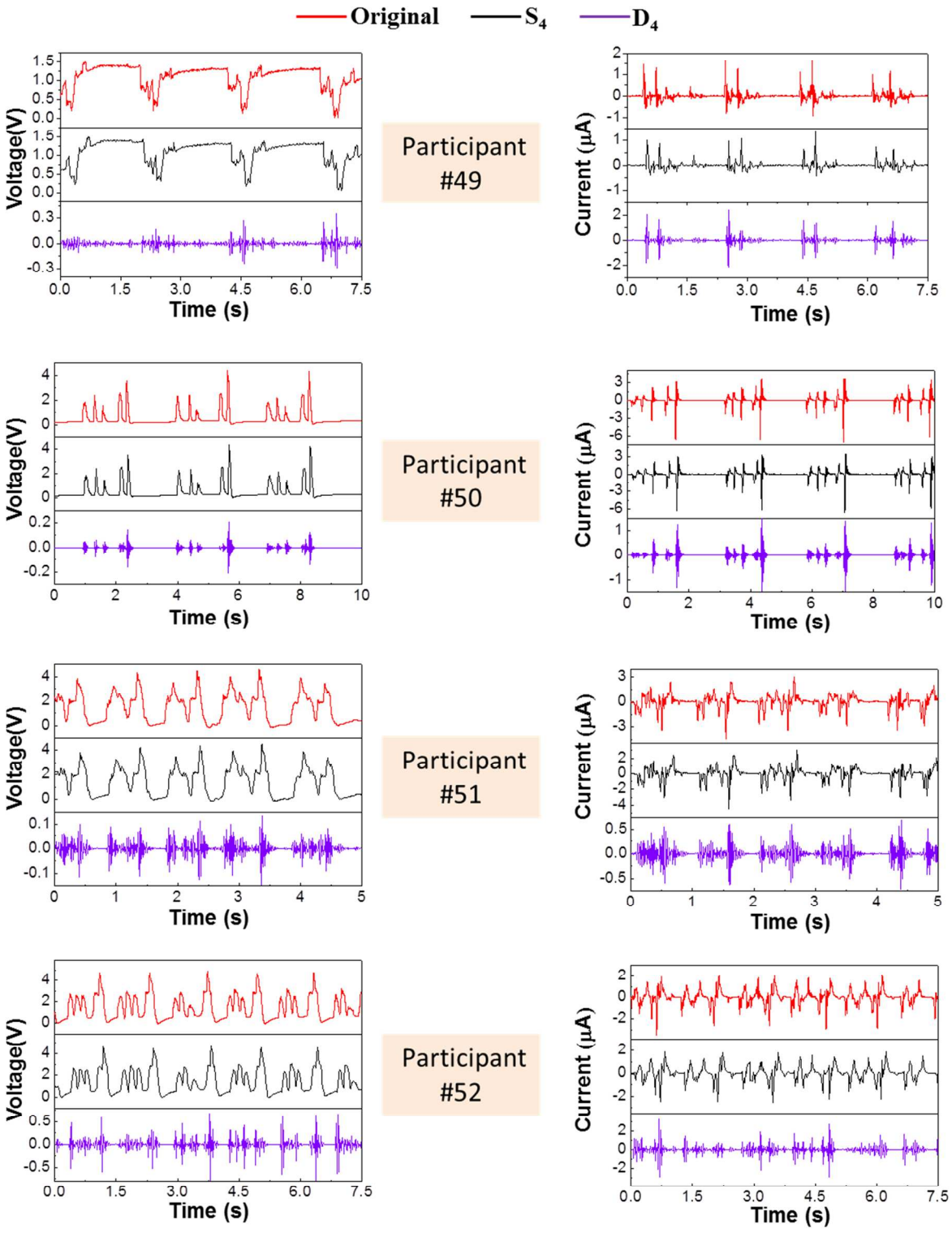

Supporting Figure S19 | The typing patterns of participants 49 to 52. Typing patterns obtained when they were continuously tying the word "touch" into the computer *via* the IKB. S_4 and D_4 are the corresponding wavelet components after DB4 transformation.

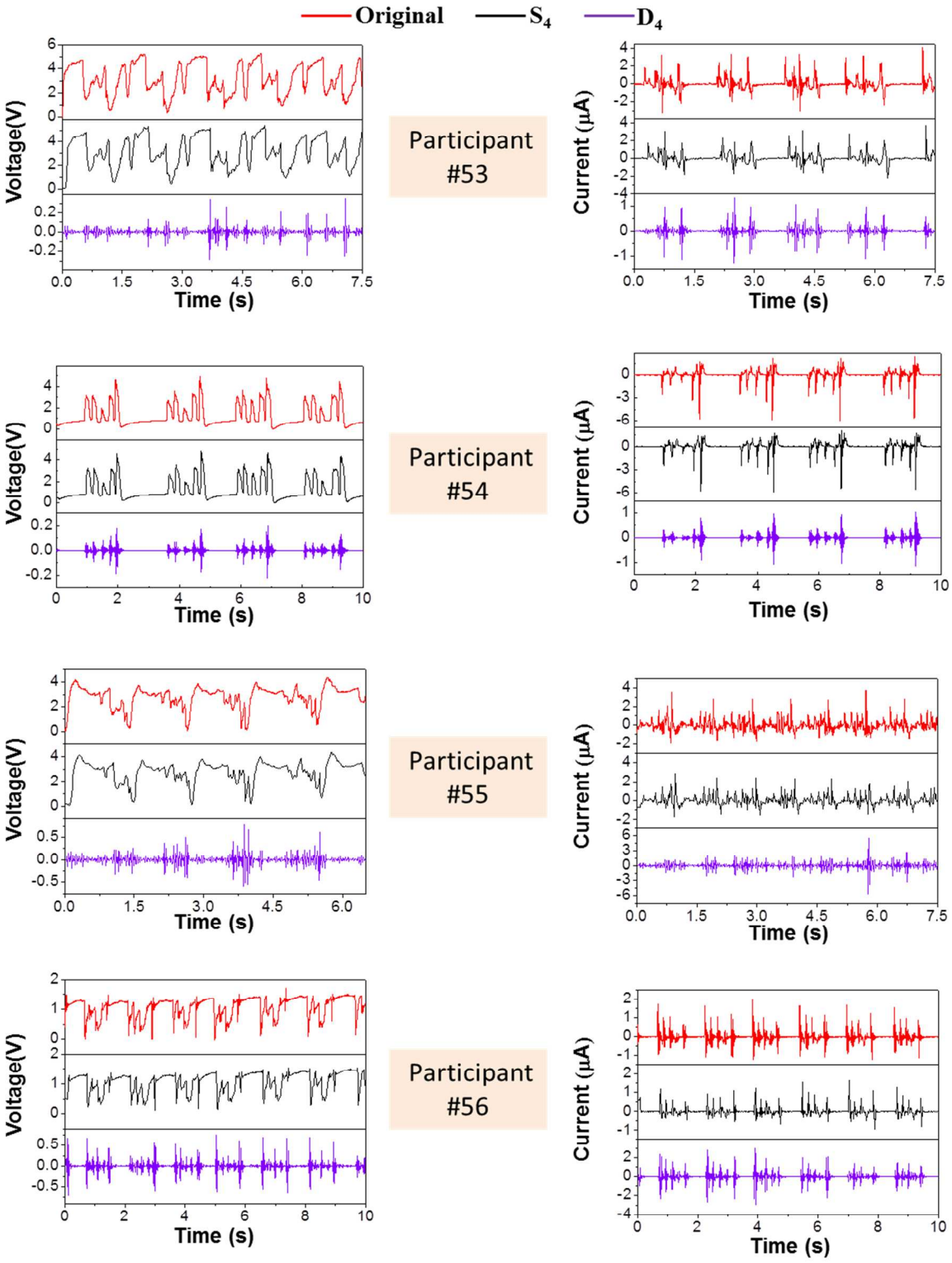

Supporting Figure S20 | The typing patterns of participants 53 to 56. Typing patterns obtained when they were continuously tying the word "touch" into the computer *via* the IKB. S_4 and D_4 are the corresponding wavelet components after DB4 transformation.

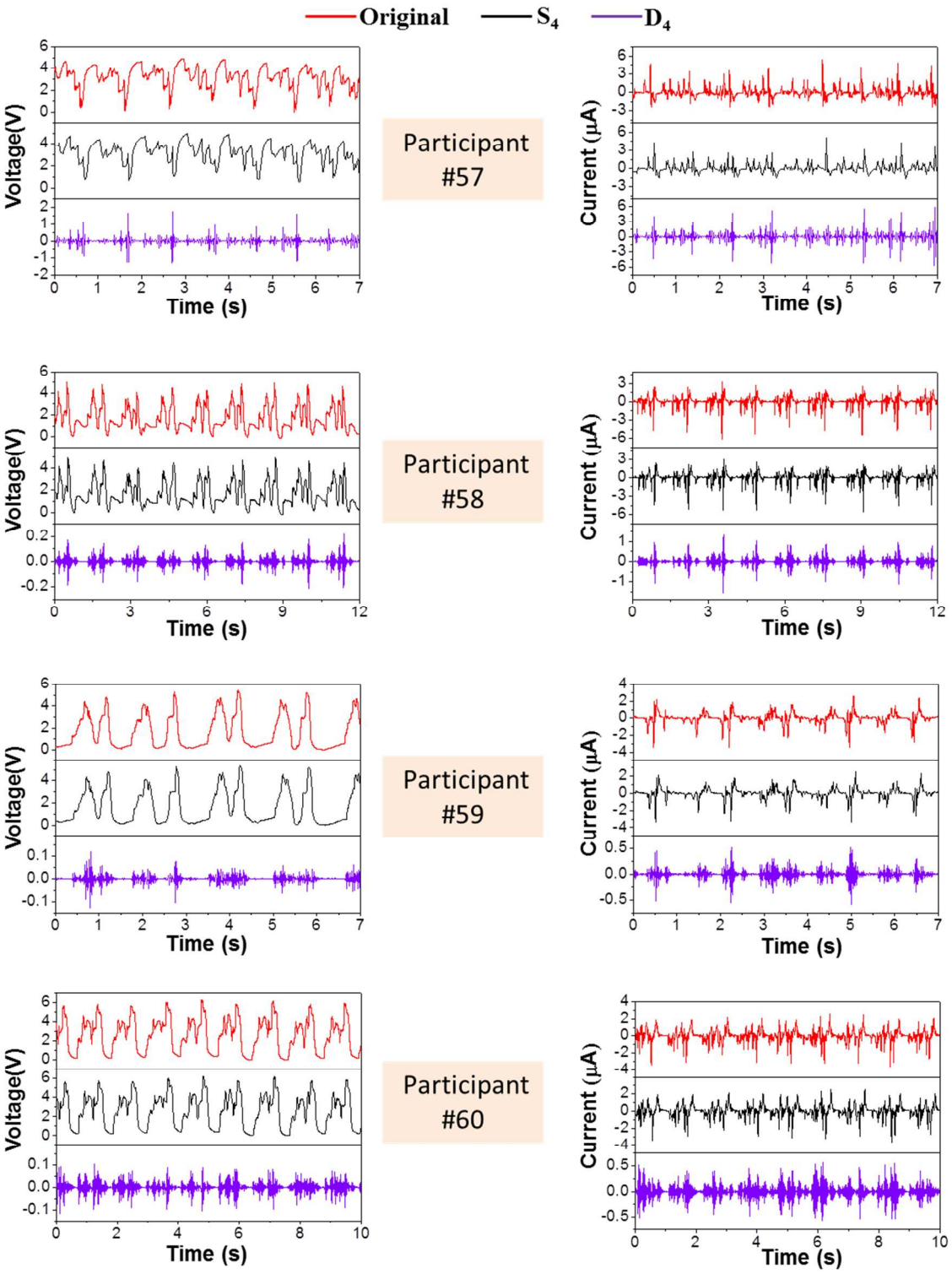

Supporting Figure S21 | The typing patterns of participants 57 to 60. Typing patterns obtained when they were continuously tying the word "touch" into the computer *via* the IKB. S_4 and D_4 are the corresponding wavelet components after DB4 transformation.

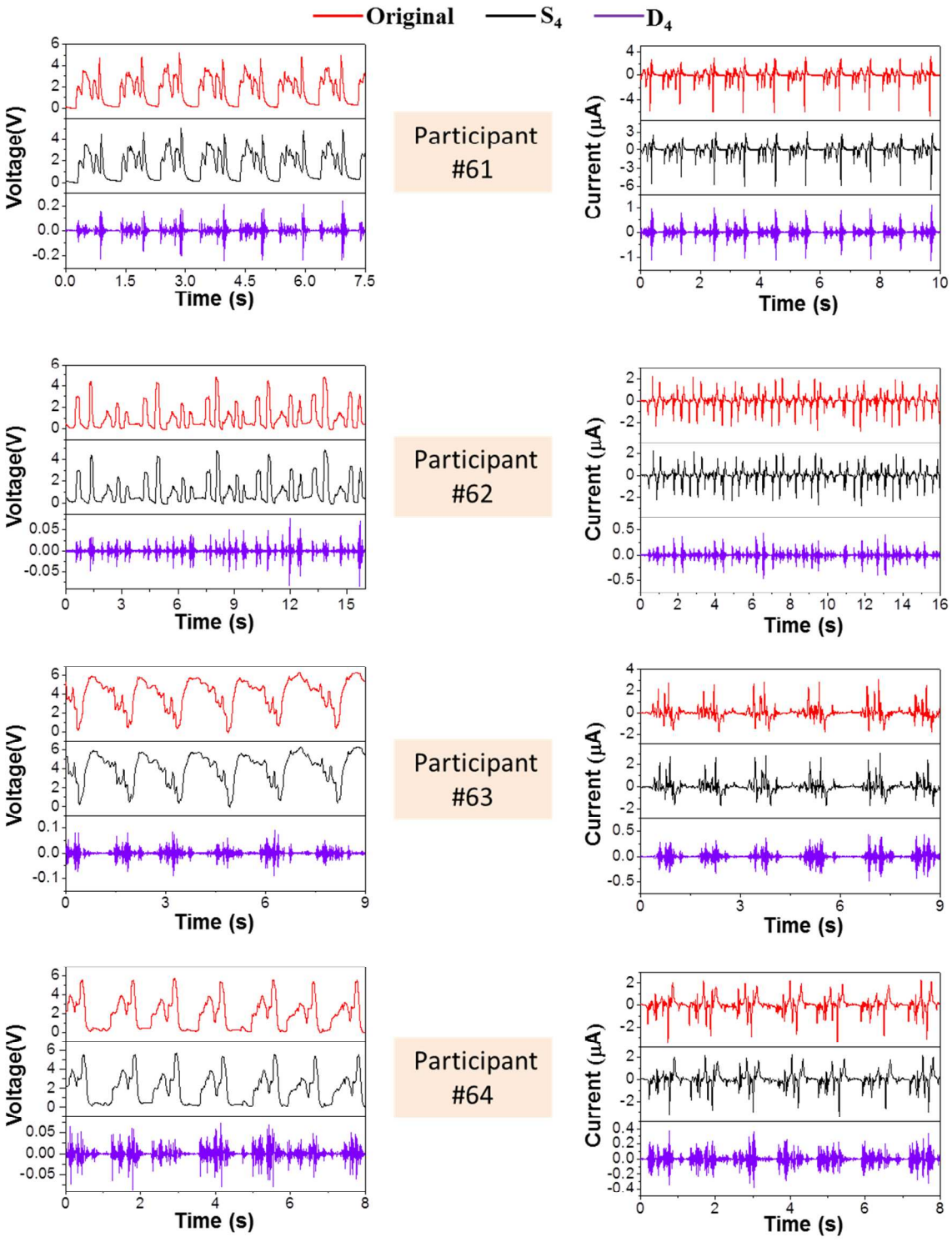

Supporting Figure S22 | The typing patterns of participants 61 to 64. Typing patterns obtained when they were continuously tying the word "touch" into the computer *via* the IKB. S_4 and D_4 are the corresponding wavelet components after DB4 transformation.

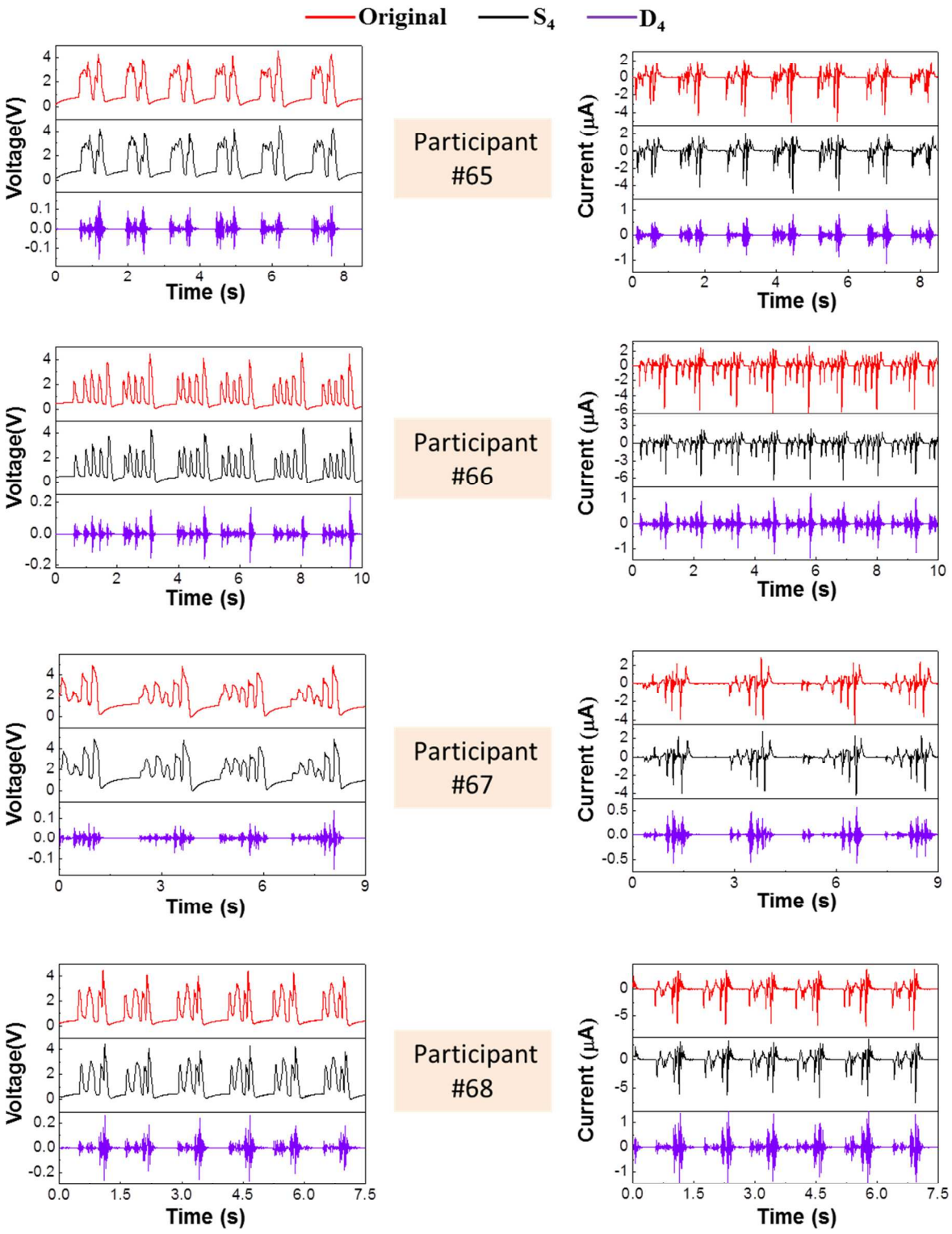

Supporting Figure S23 | The typing patterns of participants 65 to 68. Typing patterns obtained when they were continuously tying the word "touch" into the computer *via* the IKB. S_4 and D_4 are the corresponding wavelet components after DB4 transformation.

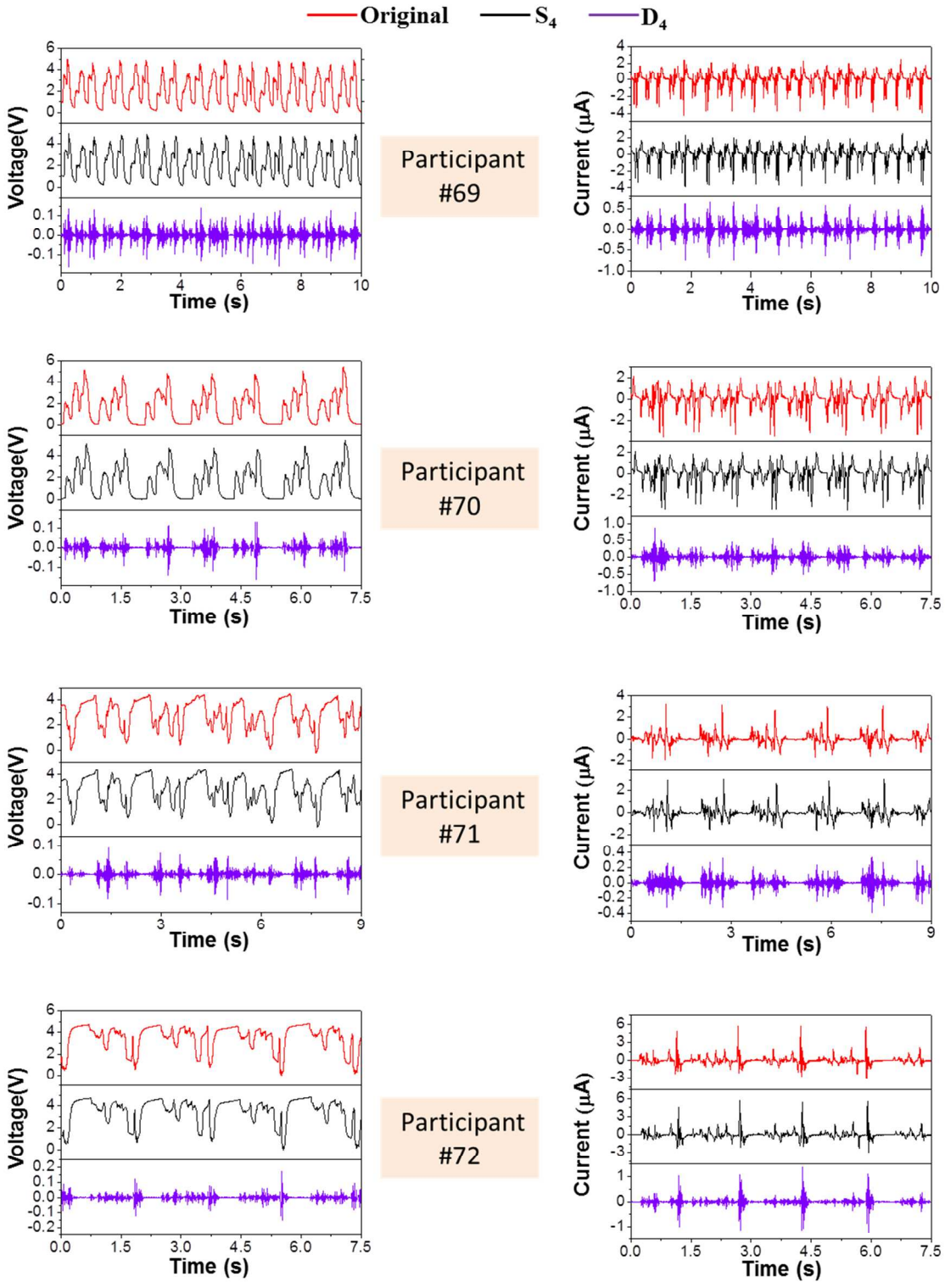

Supporting Figure S24 | The typing patterns of participants 69 to 72. Typing patterns obtained when they were continuously tying the word "touch" into the computer *via* the IKB. S_4 and D_4 are the corresponding wavelet components after DB4 transformation.

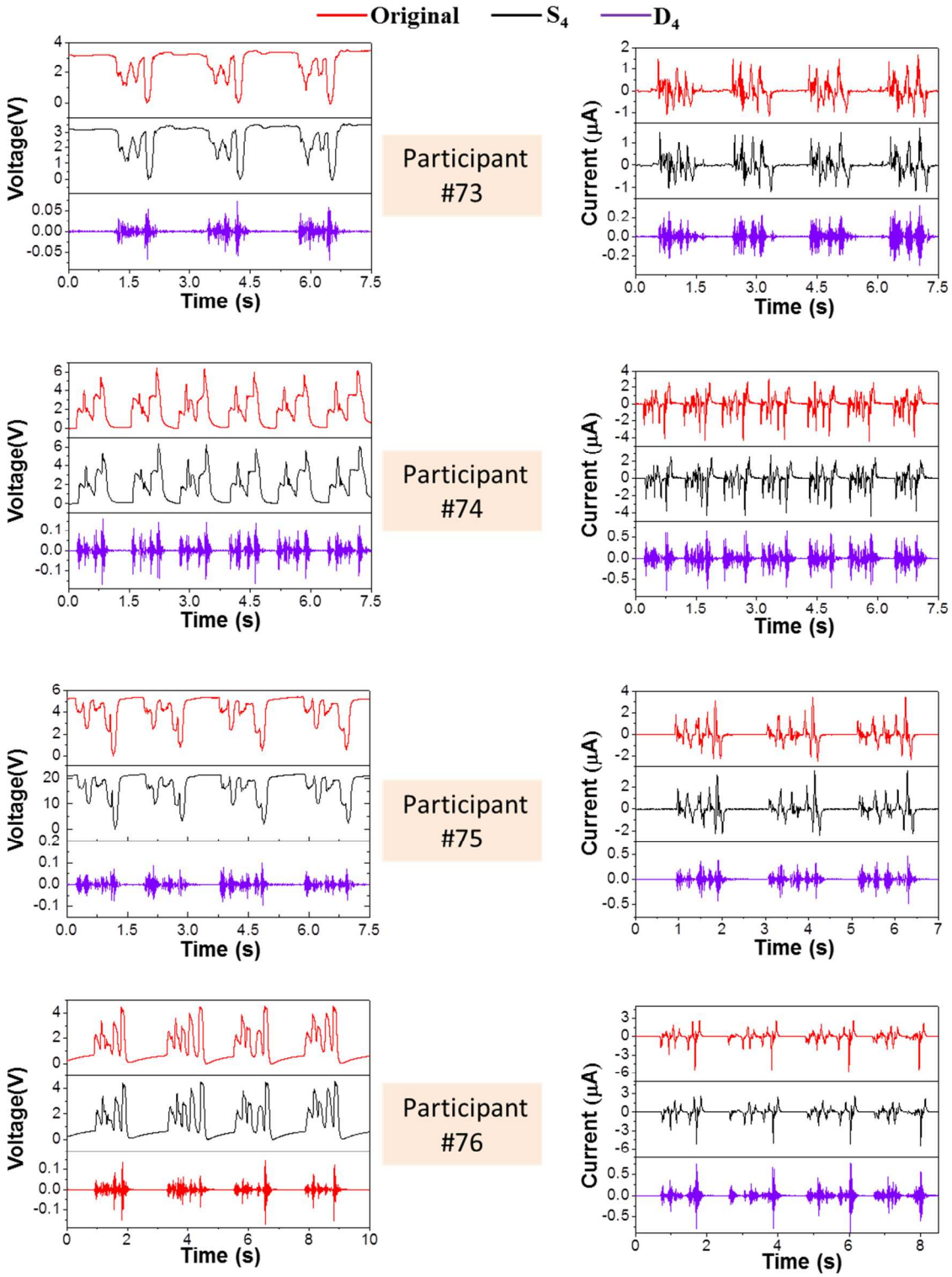

Supporting Figure S25 | The typing patterns of participants 73 to 76. Typing patterns obtained when they were continuously tying the word "touch" into the computer *via* the IKB. S_4 and D_4 are the corresponding wavelet components after DB4 transformation.

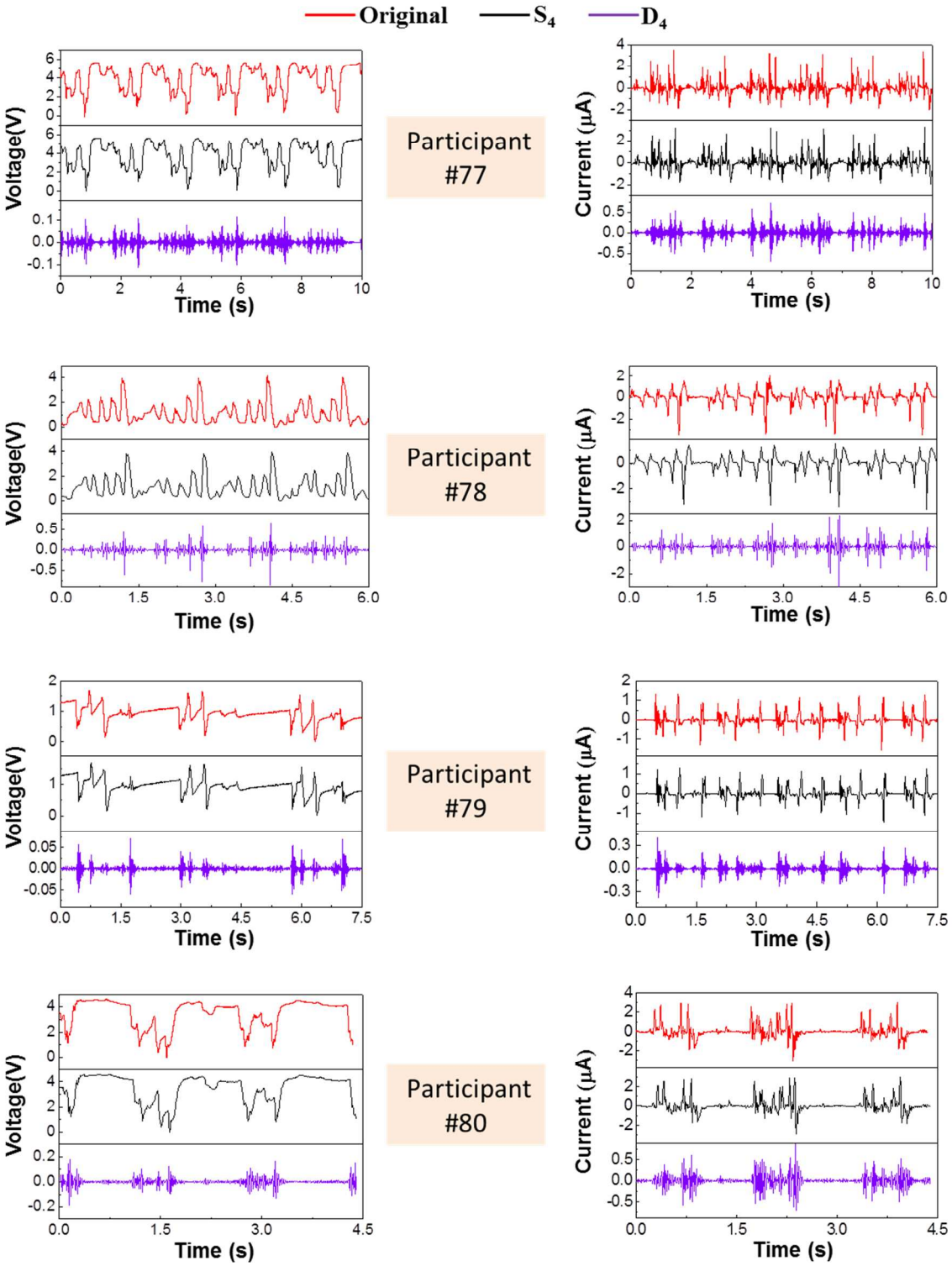

Supporting Figure S26 | The typing patterns of participants 77 to 80. Typing patterns obtained when they were continuously tying the word "touch" into the computer *via* the IKB. S_4 and D_4 are the corresponding wavelet components after DB4 transformation.

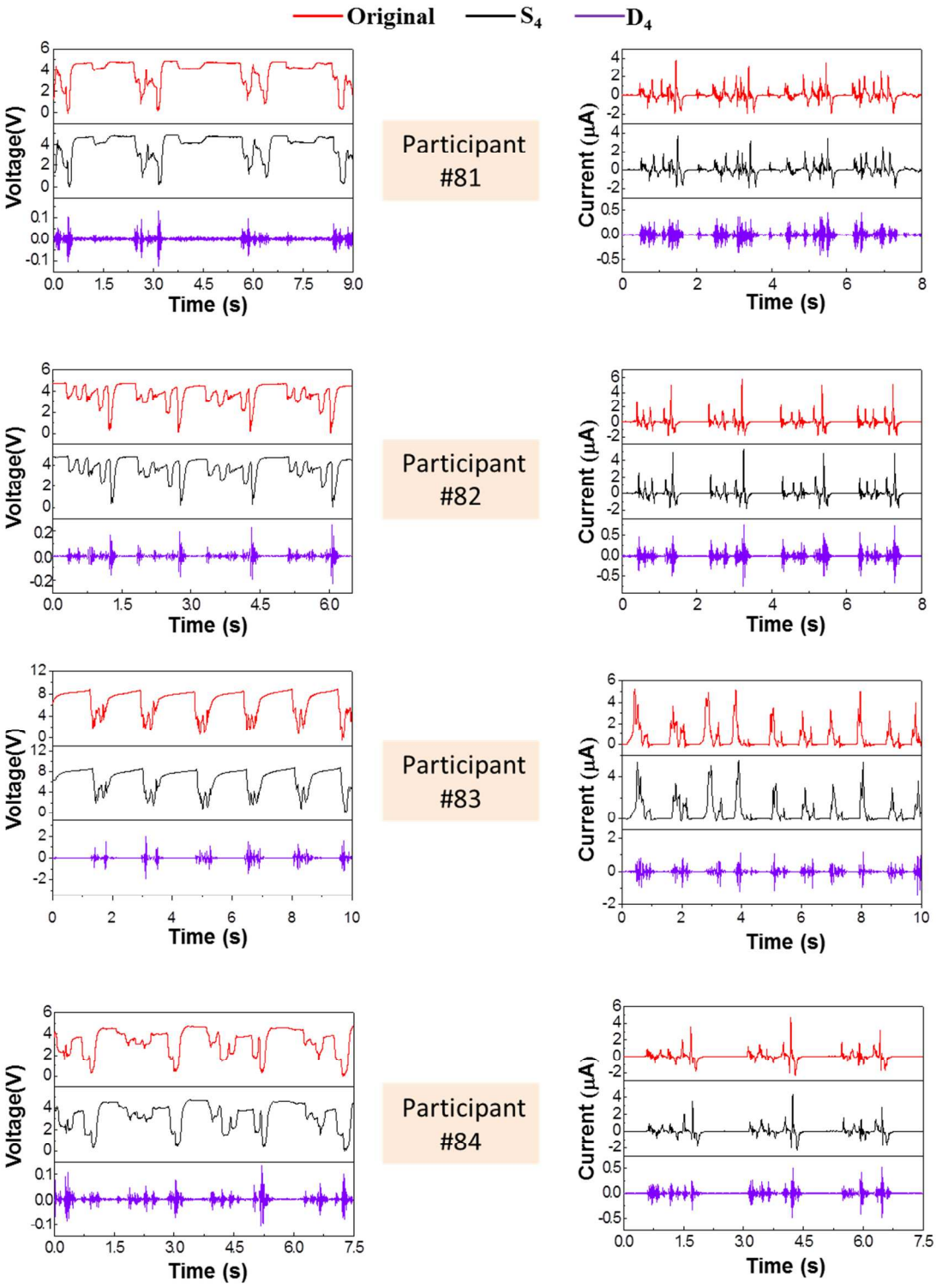

Supporting Figure S27 | The typing patterns of participants 81 to 84. Typing patterns obtained when they were continuously tying the word "touch" into the computer *via* the IKB. S_4 and D_4 are the corresponding wavelet components after DB4 transformation.

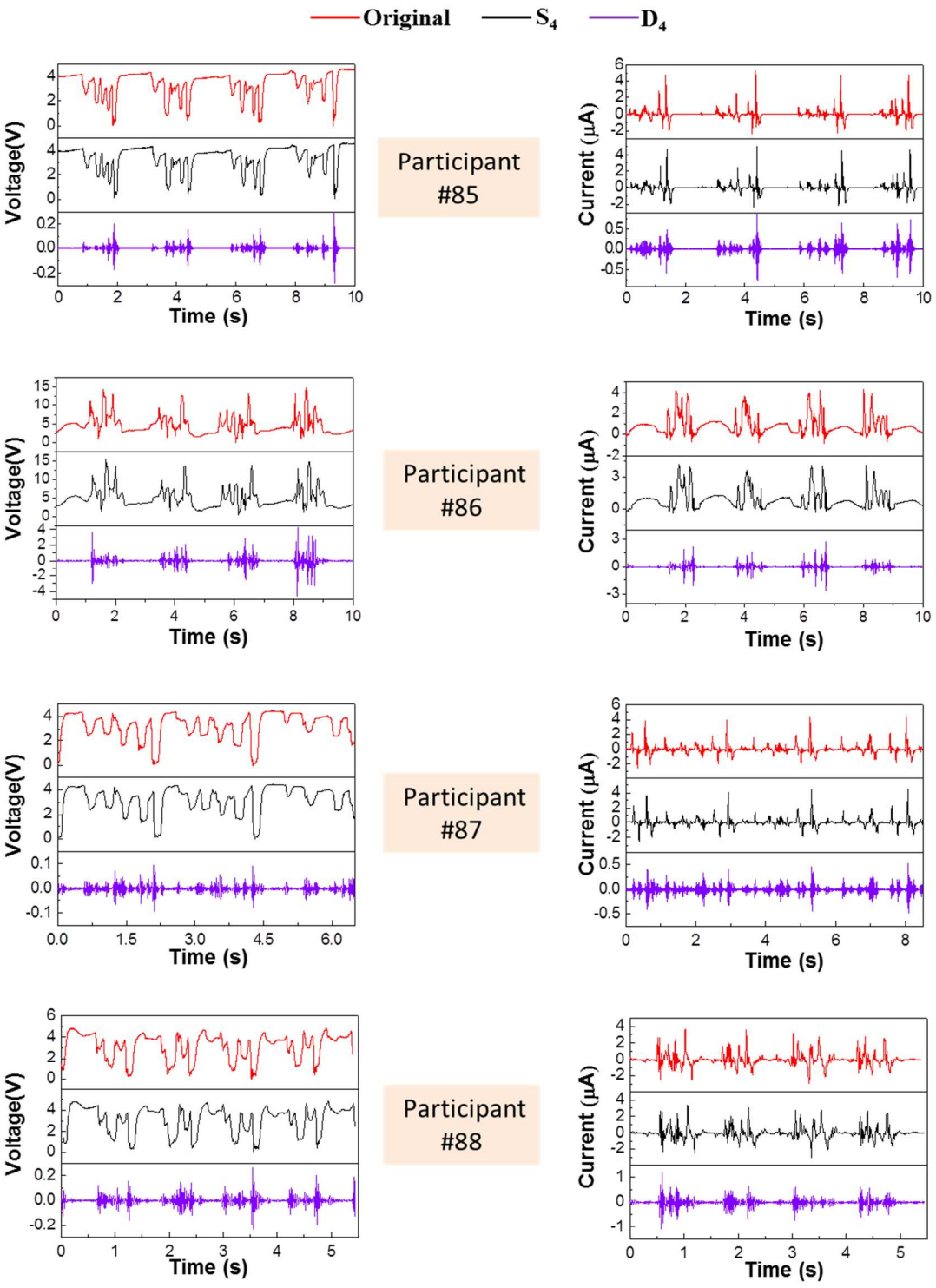

Supporting Figure S28 | The typing patterns of participants 85 to 88. Typing patterns obtained when they were continuously tying the word "touch" into the computer *via* the IKB. S_4 and D_4 are the corresponding wavelet components after DB4 transformation.

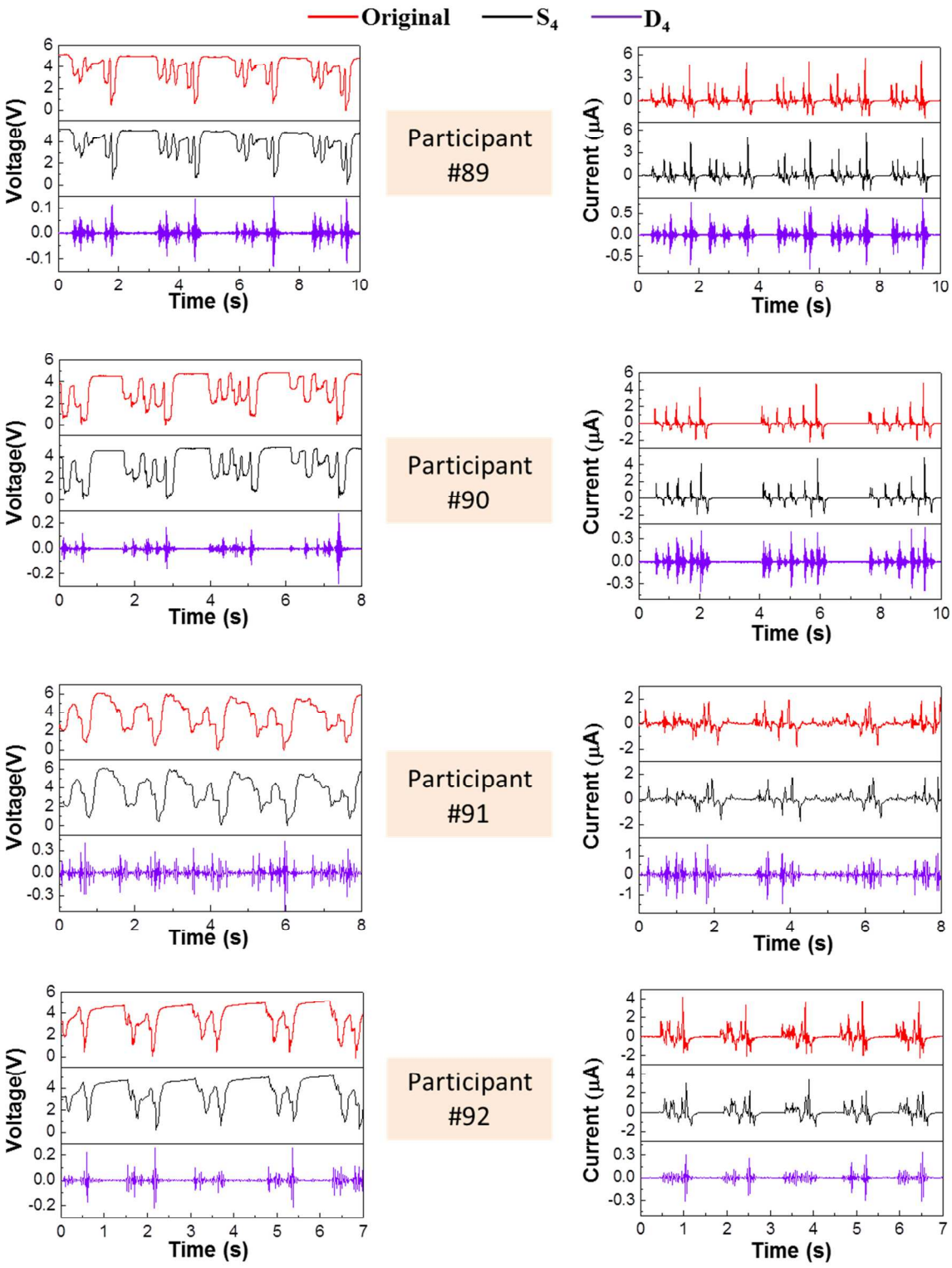

Supporting Figure S29 | The typing patterns of participants 89 to 92. Typing patterns obtained when they were continuously tying the word "touch" into the computer *via* the IKB. S_4 and D_4 are the corresponding wavelet components after DB4 transformation.

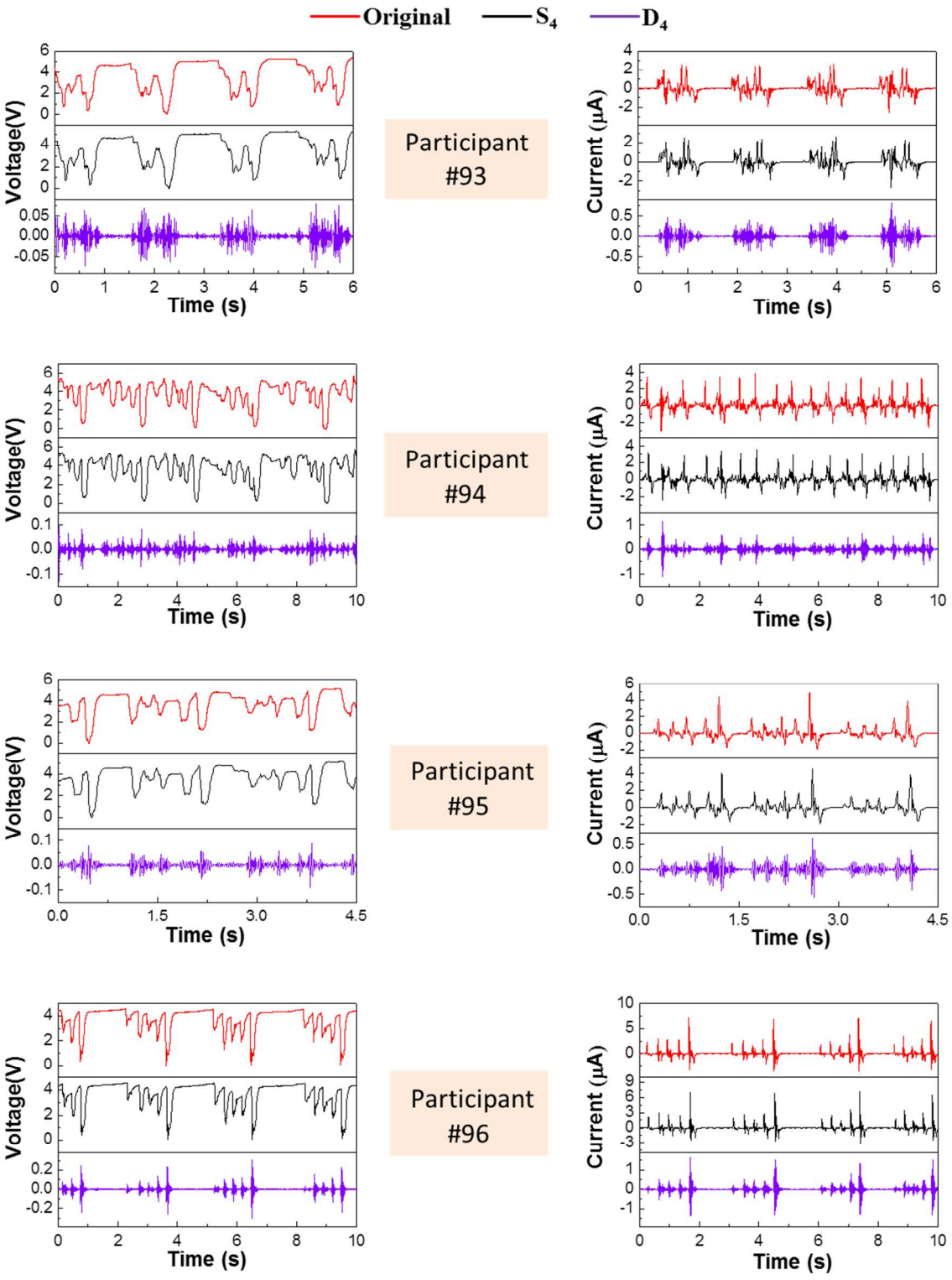

Supporting Figure S30 | The typing patterns of participants 93 to 96. Typing patterns obtained when they were continuously tying the word "touch" into the computer *via* the IKB. S_4 and D_4 are the corresponding wavelet components after DB4 transformation.

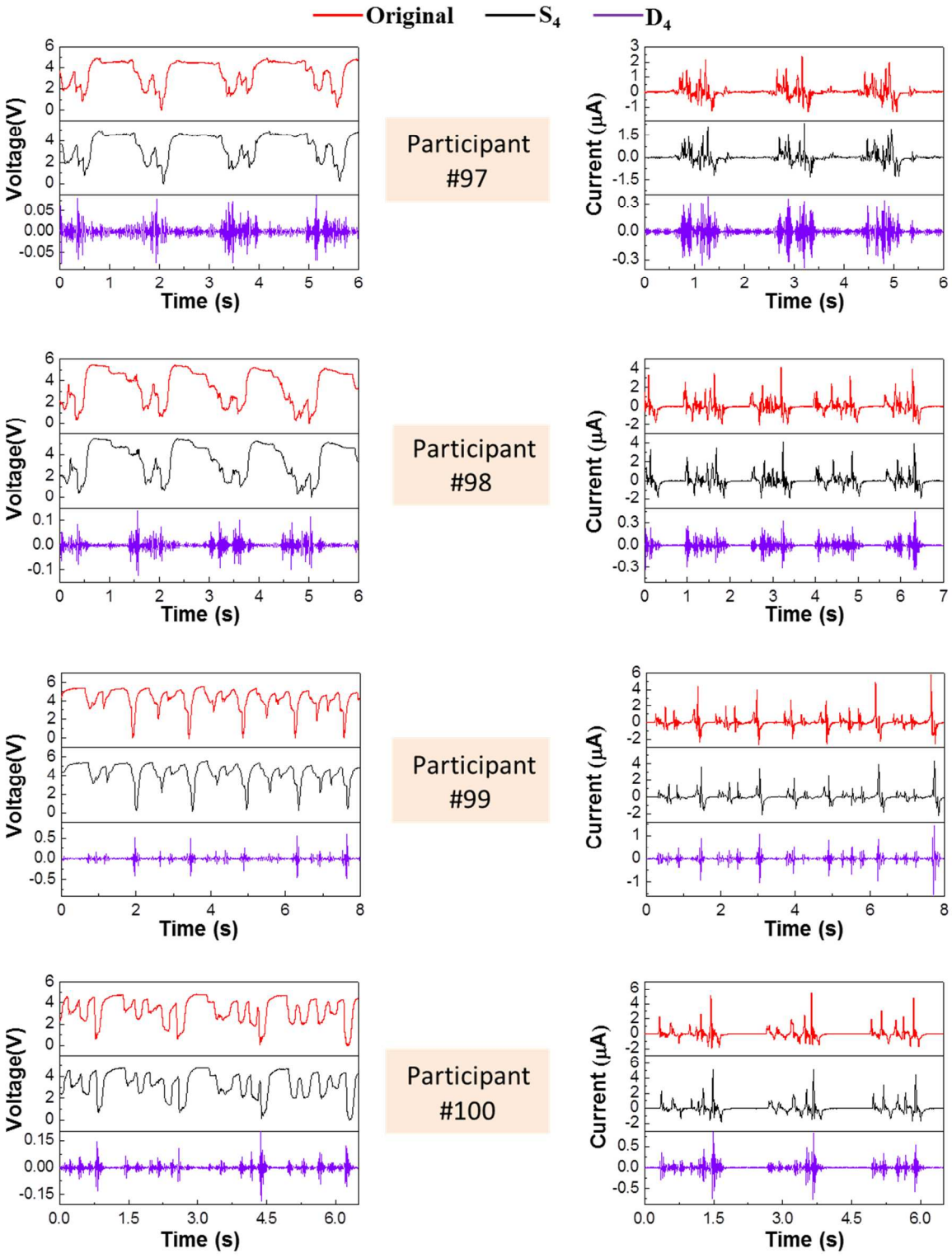

Supporting Figure S31 | The typing patterns of participants 97 to 100. Typing patterns obtained when they were continuously tying the word "touch" into the computer *via* the IKB. S_4 and D_4 are the corresponding wavelet components after DB4 transformation.

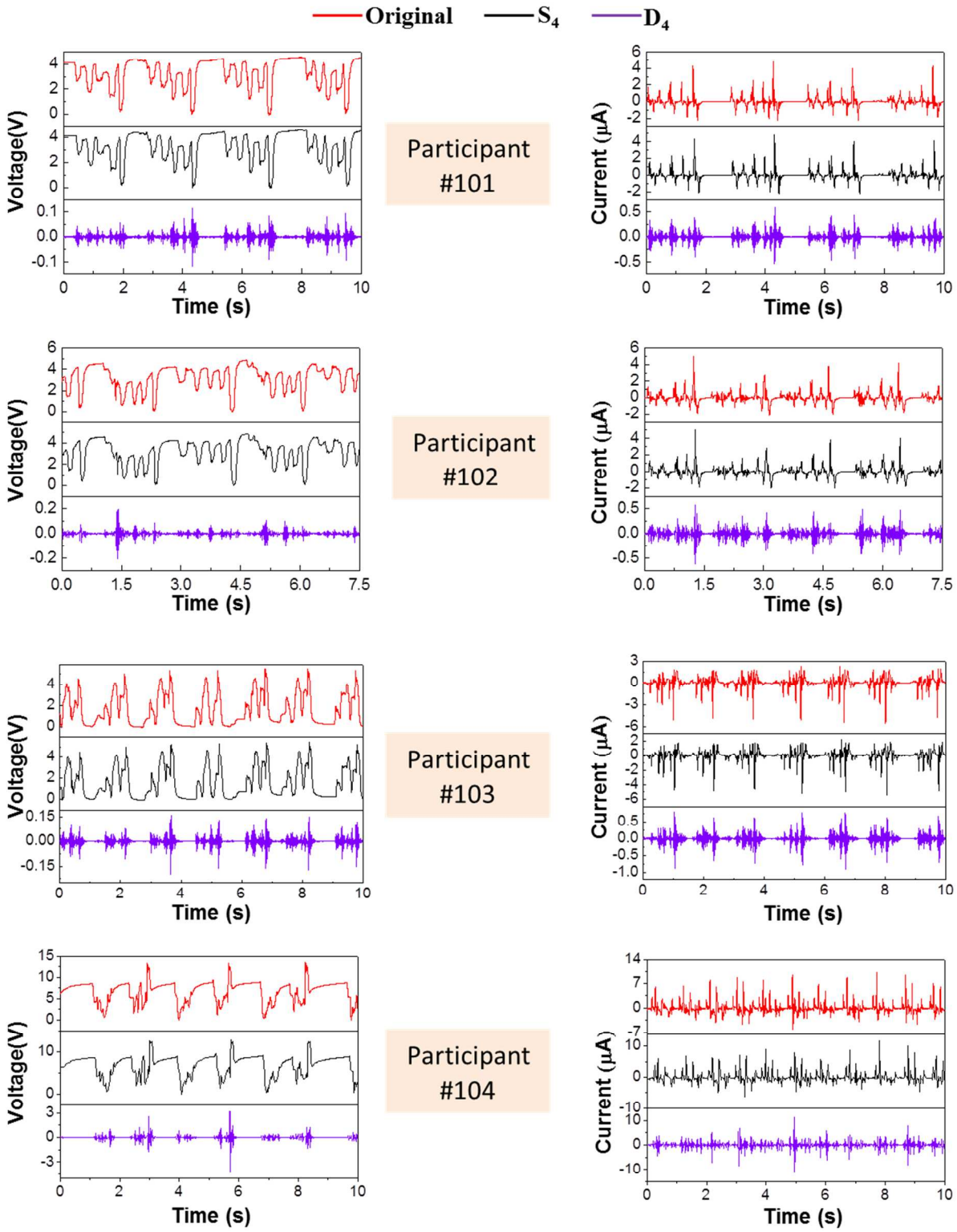

Supporting Figure S32 | The typing patterns of participants 101 to 104. Typing patterns obtained when they were continuously tying the word "touch" into the computer *via* the IKB. S_4 and D_4 are the corresponding wavelet components after DB4 transformation.

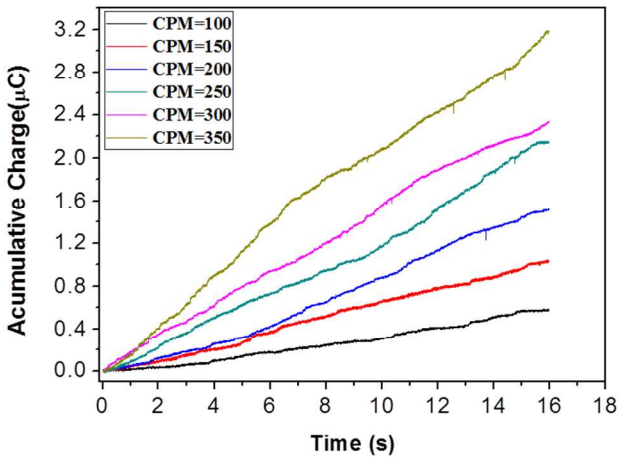

Supporting Figure S33 | Accumulative triboelectric charges by the intelligent keyboard under the continuous typing work model. A directly proportional relationship was found between the typing speed and the charge accumulative rate, which is because a faster typing means more keystrokes are launched in a unit period of time, and thus a faster of triboelectric charges generation is expected.

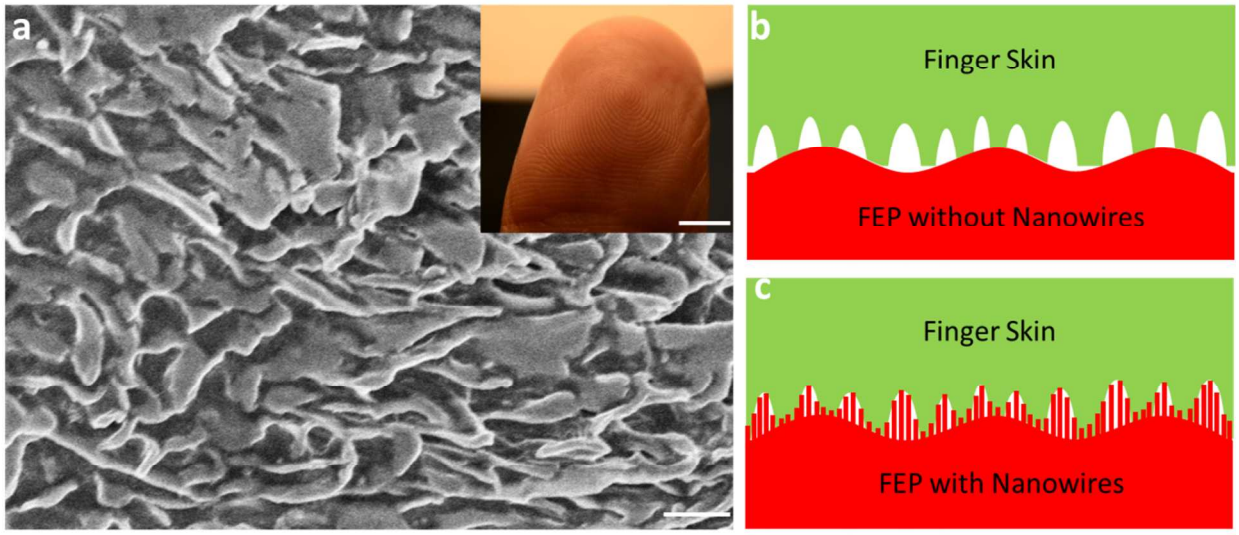

Supporting Figure S34 | Contact area was improved by FEP nanowires surface modification. (**a**) SEM image of human finger skin. (Scale bar,1 μm). Inset: photograph of a human finger surface (scale bar, 0.5 cm). (**b**) Illustration of the surface contact area between human finger skin and FEP without nanowires modification when a keystroke was applied. (**c**) Illustration of the surface contact area between human finger skin and nanowires-modified FEP surface when a keystroke was initiated.

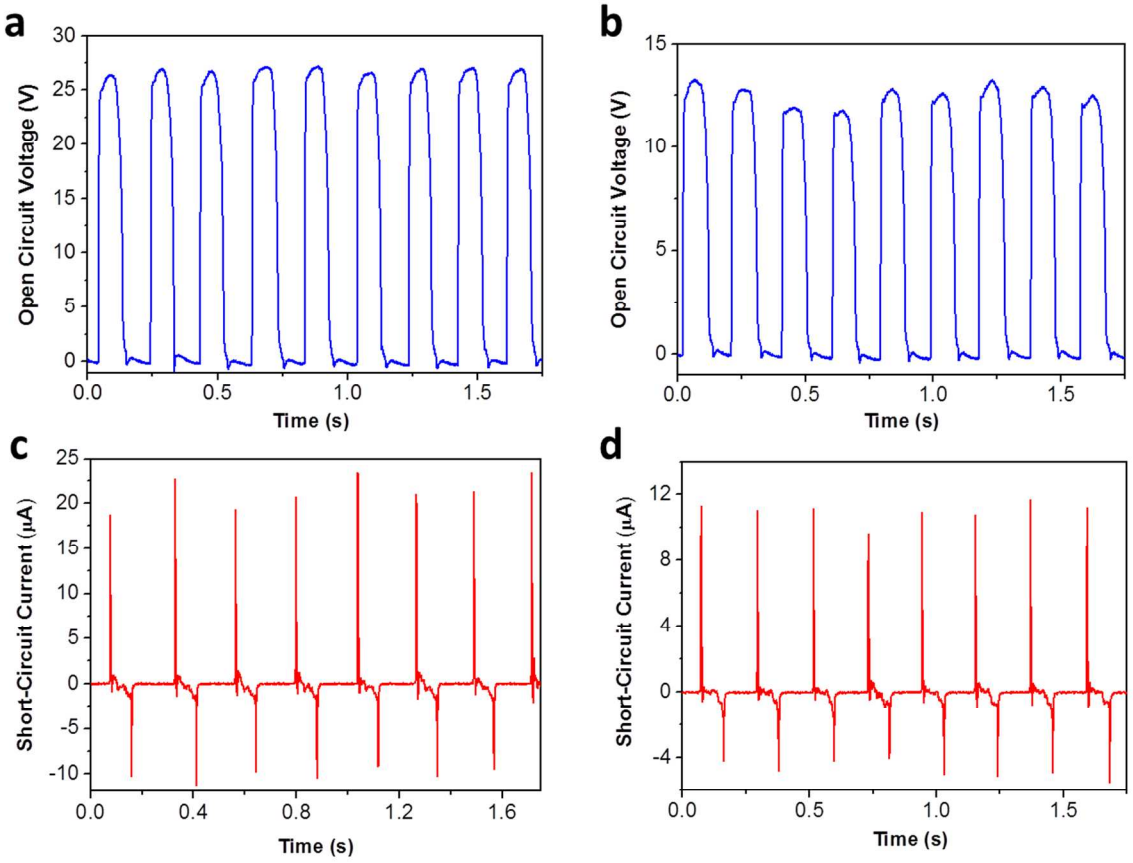

Supporting Figure S35 | Electrical output comparison of an IKB in the intermittent tying mode with or without FEP nanowires surface modification. Open-circuit voltage of the IKB with (**a**) and without (**b**) FEP nanowires when a key in zone "II" was repeatedly tested. Short-circuit current of the IKB with (**c**) and without (**d**) FEP nanowires when a key in zone "II" was repeatedly tested.

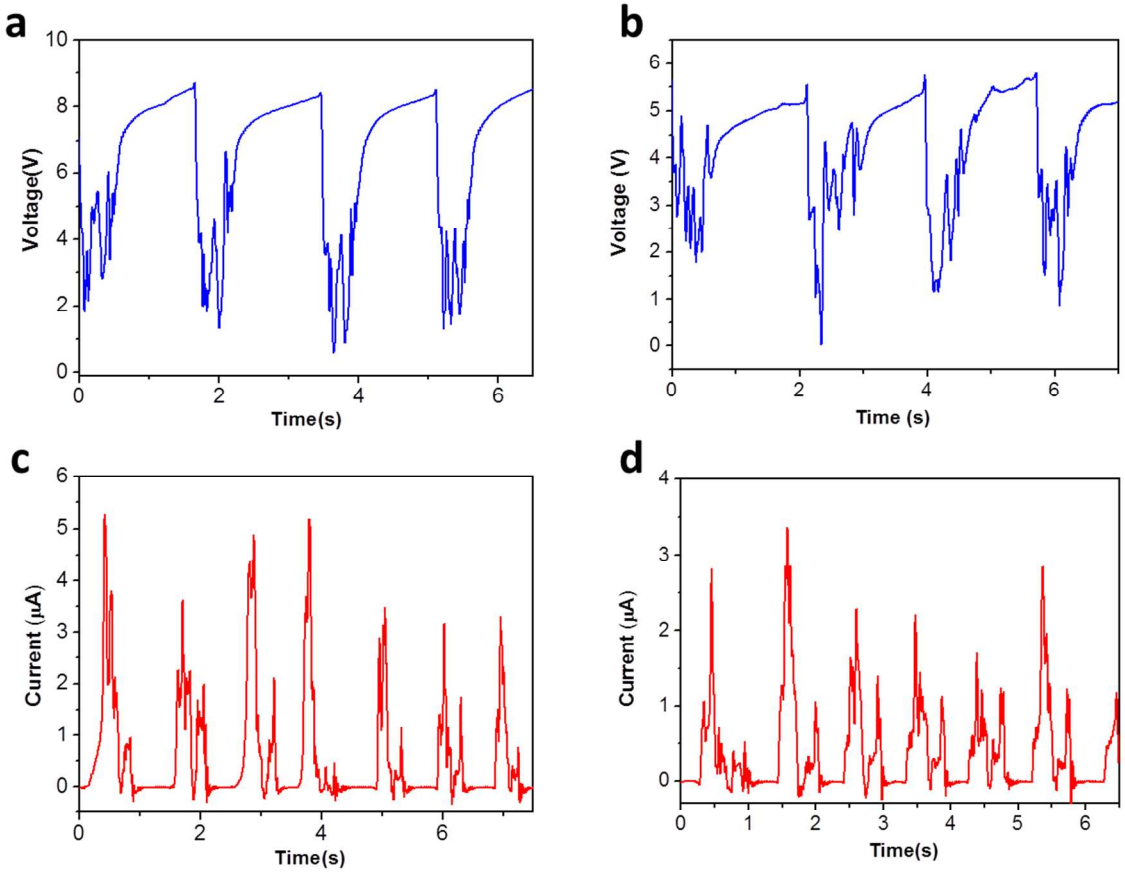

Supporting Figure S36 | Electrical output comparison of an IKB in the continuously typing mode with or without FEP nanowires surface modification. Obtained voltage signals of the IKB with (**a**) and without (**b**) FEP nanowires when Tom independently typed the word "touch" for more than three times on the IKB in his accustomed manner. Current output of the IKB with (**c**) and without (**d**) FEP nanowires when Tom independently typed the word "touch" for more than three times on the IKB in his accustomed manner.

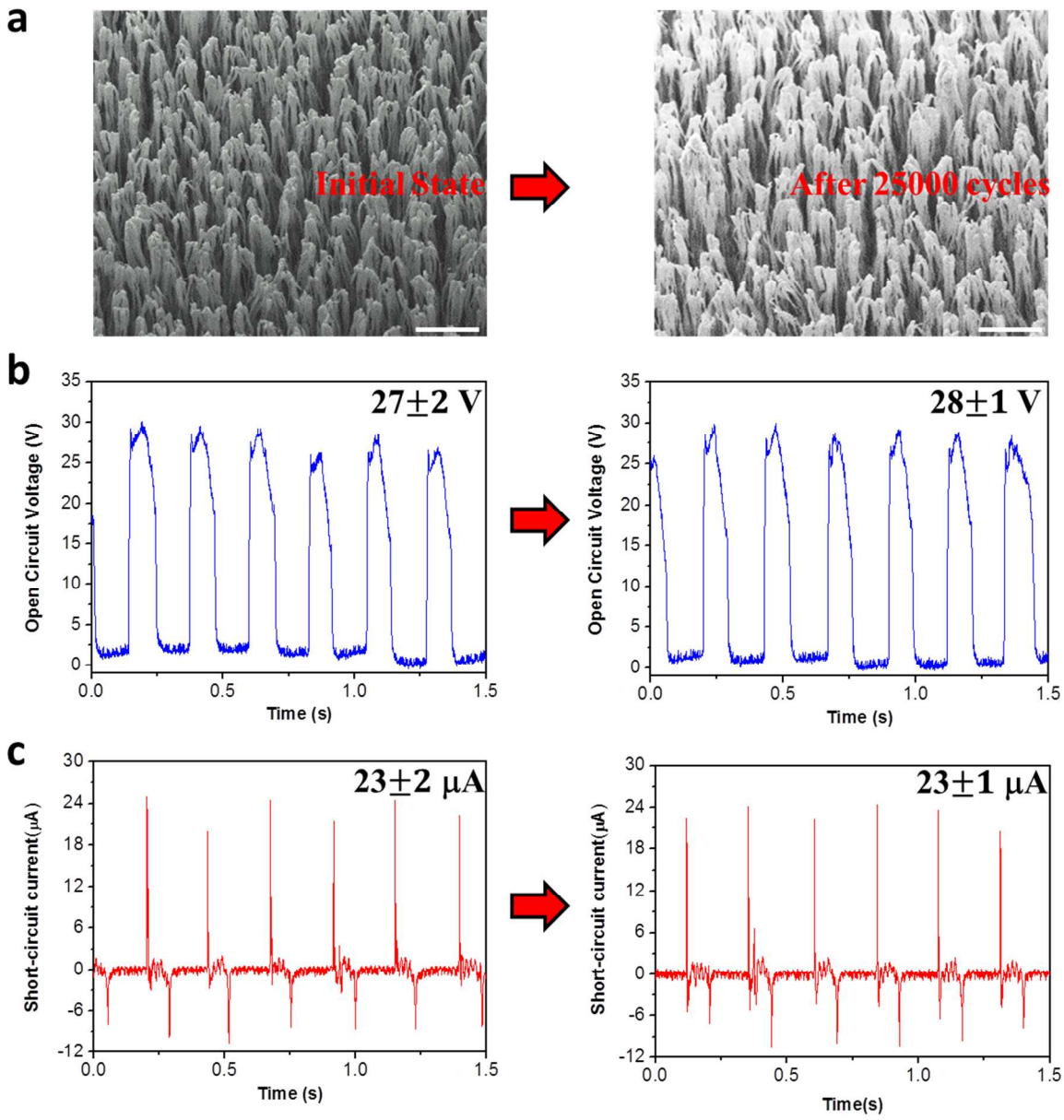

Supporting Figure S37 | IKB mechanical robustness investigation. (a) SEM images of the FEP nanowires before (left pair) and after (right pair) the finger keystroke for 25000 cycles at an applied force at 2.3 ± 0.2 N. All the scale bars are 500 nm. Open circuit voltage (**b**) and short-circuit current (**c**) of the IKB before (left pair) and after (right pair) the keystroke for 25000 cycles, when the "II" keys was stroked by an index finger with an applied force at 2.3 ± 0.2 N.

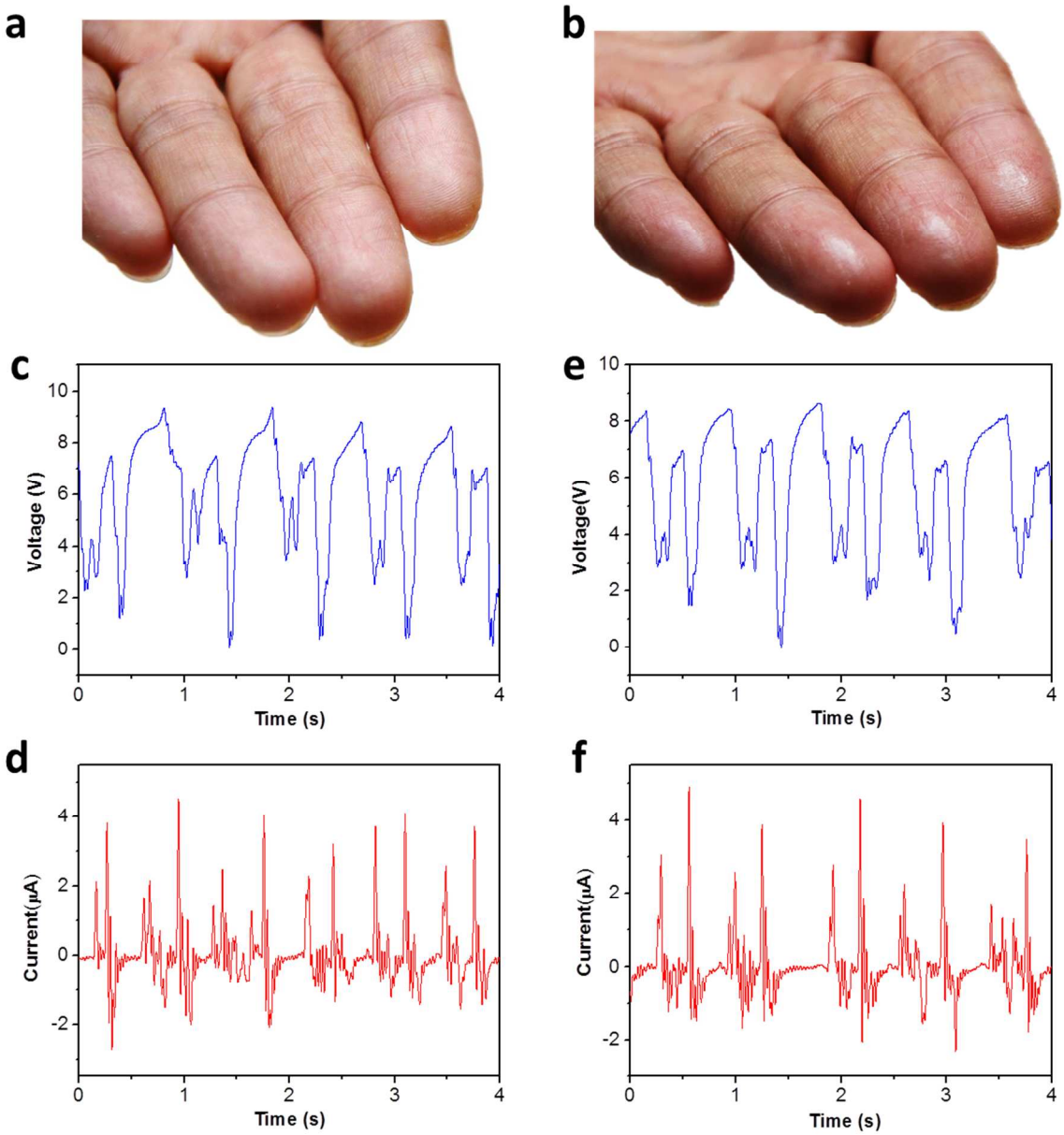

Supporting Figure S38 | The influence of sweaty hand on the IKB output performance. (a) A photograph of John's clean hand. (**b**) A photograph of the hand after a long-distance running, which was naturally getting sweaty. Typing patter of John, (**c**) voltage and (**d**) current, when he typed the word "touch" for more than four times on the IKB in his accustomed manner with his clean hand. Typing patter of John, (**e**) voltage and (**f**) current, when he typed the word "touch" for more than four times on the IKB in his accustomed manner with his sweaty hand after a long-distance running.

Supporting Table S1| Major components of frequency spectrum of typing patterns.

	Tom	Mike	Alex
Voltage Data	[0.4, 4, 6.2, 8.7]	[0.41, 1.25, 3, 5, 6.6, 9]	[1.25, 2.5, 3.3, 7.5]
Current Data	[1.25, 2.1, 3.3, 4.2, 9.6]	[0.81, 2.1, 3.75, 5, 6.2, 7.5,8.75]	[1.2, 3.3, 4.6, 5.4, 7.9, 9.2]

Supporting Table S2 | Triboelectric table (Tests were performed by Bill Lee (Ph.D., physics). ©2009 by AlphaLab, Inc. (TriField.com), which also manufactured the test equipment used.) Column 1: Insulator name. Column 2: Charge affinity in nC/J. Column 3: Notes.

Human hand, oily skin	+45	Skin is conductive. Cannot be charged by metal rubbing.
Solid polyurethane, filled	+40	Slightly conductive. (8 T ohm cm).
Magnesium fluoride (MgF2)	+35	Anti-reflective optical coating.
Nylon	+30	
Machine oil	+29	
Nylatron (nylon filled with MoS_2)	+28	
Glass (soda)	+25	Slightly conductive. (Depends on humidity).
Paper (uncoated copy)	+10	Slightly conductive.
Wood (pine)	+7	
GE brand Silicone II (hardens in air)	+6	More positive than the other silicone chemistry.
Cotton	+5	Slightly conductive. (Depends on humidity).
Nitrile rubber	+3	
Wool	0	
Polycarbonate	-5	
ABS	-5	
Acrylic (polymethyl methacrylate)	-10	
Epoxy (circuit board)	-32	
Styrene-butadiene rubber (SBR, Buna S)	-35	Sometimes inaccurately called "neoprene" (see below).
Solvent-based spray paints	-38	May vary.
PET (mylar) cloth	-40	
PET (mylar) solid	-40	
EVA rubber for gaskets, filled	-55	Filled rubber will usually conduct.
Gum rubber	-60	Barely conductive. (500 T ohm cm).
Hot melt glue	-62	
Polystyrene	-70	
Polyimide	-70	
Silicones (air harden & thermoset, but *not* GE)	-72	
Vinyl: flexible (clear tubing)	-75	
Carton-sealing tape (BOPP)	-85	Raw surface is very +, but close to PP when sanded.
Olefins (alkenes): LDPE, HDPE, PP	-90	UHMWPE is below.

Cellulose nitrate	-93	
Office tape backing	-95	
UHMWPE	-95	
Neoprene (polychloroprene, *not* SBR)	-98	Slightly conductive if filled (1.5 T ohm cm).
PVC (rigid vinyl)	-100	
Latex (natural) rubber	-105	
Viton, filled	-117	Slightly conductive. (40 T ohm cm).
Epichlorohydrin rubber, filled	-118	Slightly conductive. (250 G ohm cm).
Santoprene rubber	-120	
Hypalon rubber, filled	-130	Slightly conductive. (30 T ohm cm).
Butyl rubber, filled	-135	Conductive. (900 M ohm cm). Test was done fast.
EDPM rubber, filled	-140	Slightly conductive. (40 T ohm cm).
FEP, PTFE (Teflon)	-190	Surface is fluorine atoms-- very electronegative.

Supporting Note S1 | Analytical derivation of threshold voltage V_{th}

According to Pauta Criterion Method, for a set of measured data m_{k} with k >10, if one of the data meet the following criterion

$$(\bar{m} - 3\sigma) \leq m_{\mathrm{k}} \leq (\bar{m} + 3\sigma) \tag{1}$$

where $\bar{m}$ and σ are the mean value and standard deviation of the measured data, respectively. Then m_{k} is the gross error, and should be removed from the measured data set.

Here, for our output voltage measurement, all the acquired signals from the channels corresponding to untouched keys are similar to each other, while the acquired signal from the channel corresponding to the pressed key is much larger than other acquired data, then it could be treated as a gross error, and it can be identified using the Pauta Criterion Method.

Consequently, if we assume $\bar{V}$ and σ_0 respectively are the mean value and standard deviation of the extracted maximum peak value V_{pi}, then, the threshold voltage V_{th} can be set as follows

$$V_{\mathrm{th}} = \bar{V} + 3\sigma_0 \tag{2}$$

$$\text{where } \bar{V} = \frac{1}{n}\sum_{\mathrm{i}=1}^{n} V_{\mathrm{pi}} \tag{3}$$

$$\text{and } \quad \sigma_0 = \sqrt{(V_{\mathrm{pi}} - \bar{V})^2/n} \tag{4}$$

Substitute equation (3) and (4) into (2), we can obtain

$$V_{\mathrm{th}} = \frac{1}{n}\sum_{\mathrm{i}=1}^{n} V_{\mathrm{pi}} + \frac{3}{\sqrt{n}}\sqrt{\sum_{\mathrm{i}=1}^{n} V_{\mathrm{pi}}(V_{\mathrm{pi}} - 1)} \tag{5}$$